Dust physico-chemical and optical properties

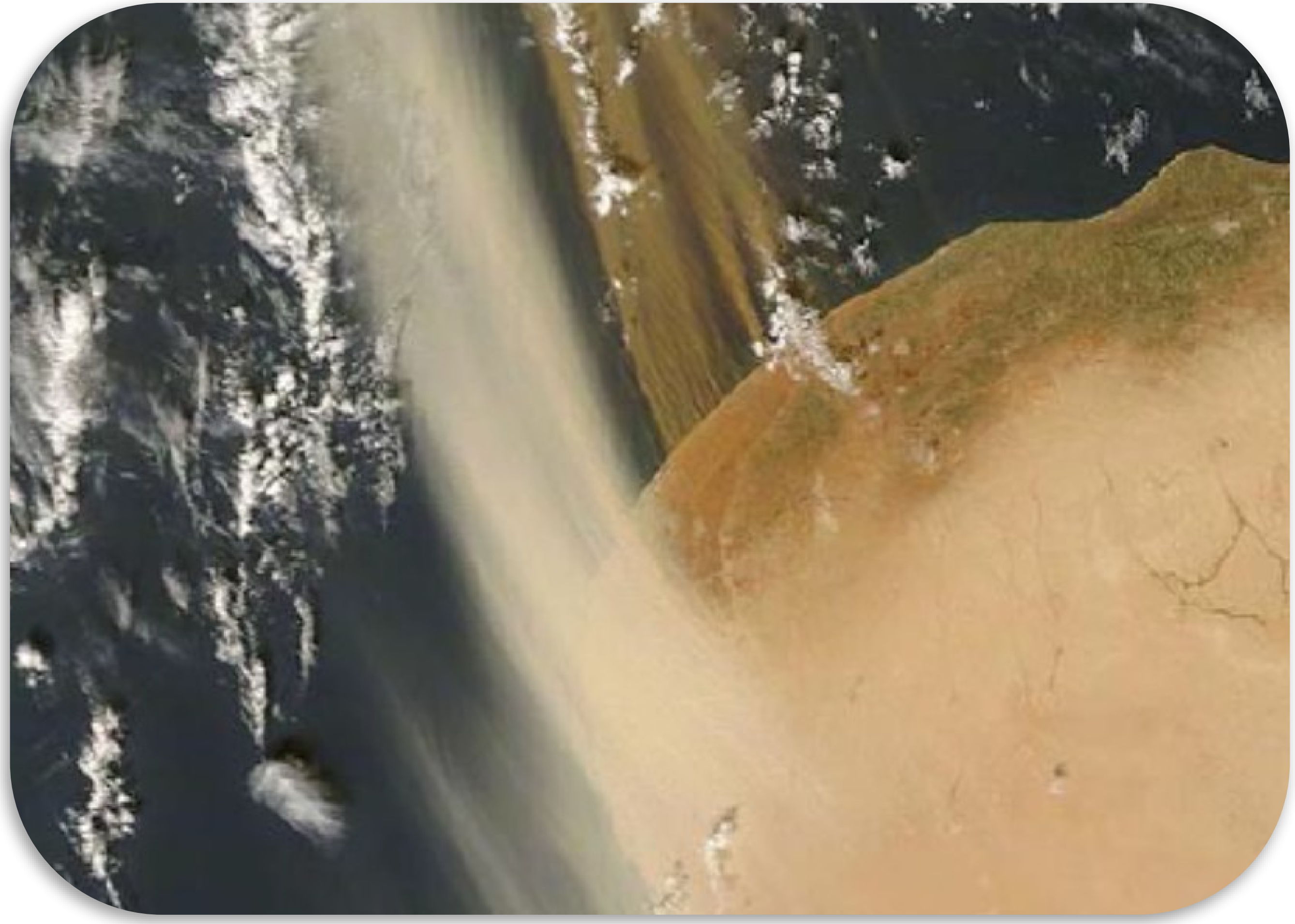

Paola Formenti

LISA, CNRS/UPEC/UP/IPSL, Créteil, France

Dust physico-chemical and optical properties

Thanks to many colleagues, of course, but above all
to **Claudia Di Biagio** and Jean-François Doussin (LISA)
Yves Balkanski (LSCE)

EUROCHAMP 2020
EFLUVE
Observatoire des Sciences de l'Univers (OSU)
lefe
Institut Pierre Simon Laplace
L-IPSL Labex
PROJET FINANCÉ PAR L'ANR - PROJECT FUNDED BY THE ANR
ANR
lisa
cnrs

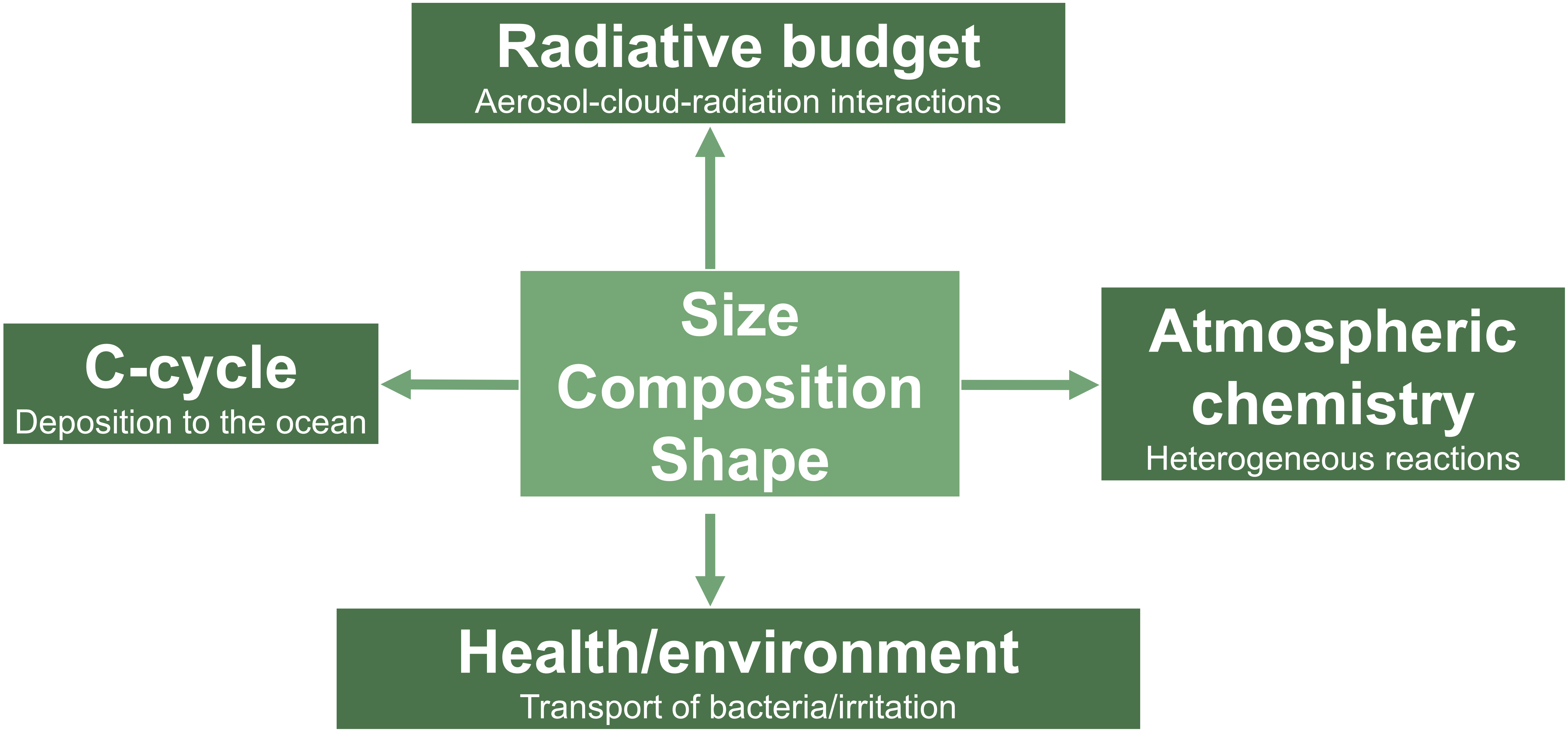

Adapted from V. Grassian

The variability issue (1/3)

Clay (aluminosilicate)

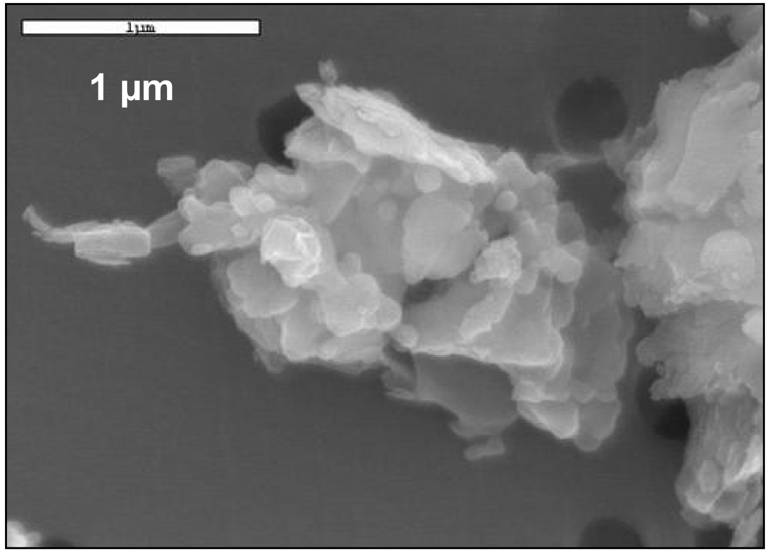

Gypsum (calcium sulphate)

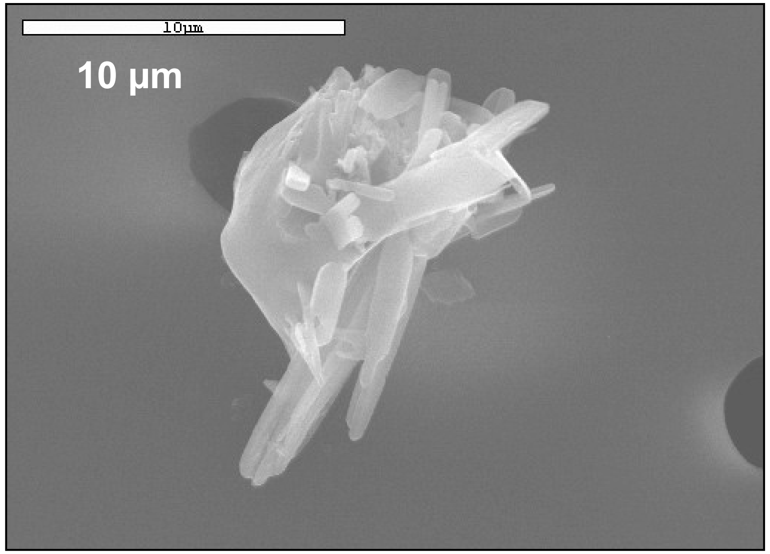

Diatomite (amorphous silicate)

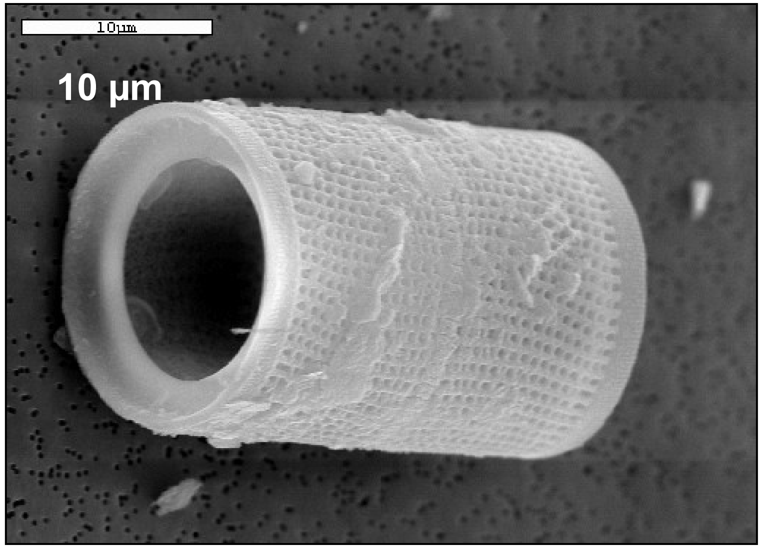

- **Size distribution**: ~ 200 nm – 20(0) µm
- **Shape**
- **Mineralogical composition**

Clays (illite, kaolinite, smectites, chlorite…), quartz, feldspaths, carbonates (calcite, dolomite), iron oxydes, others….

The variability issue (2/3)

Heterogeneous chemistry at the particle surface

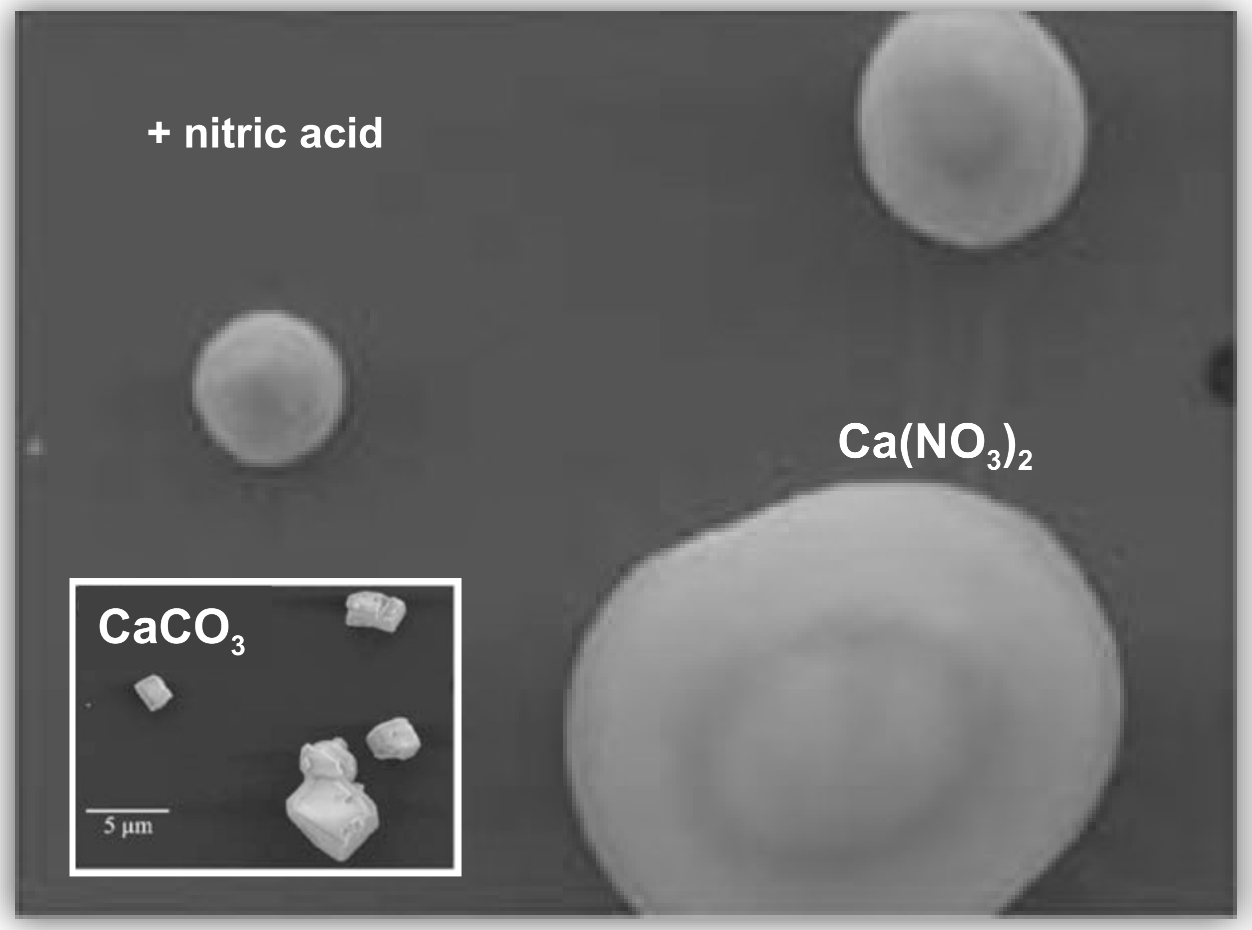

adapted from Laskin et al. (2005)

Particle mixing

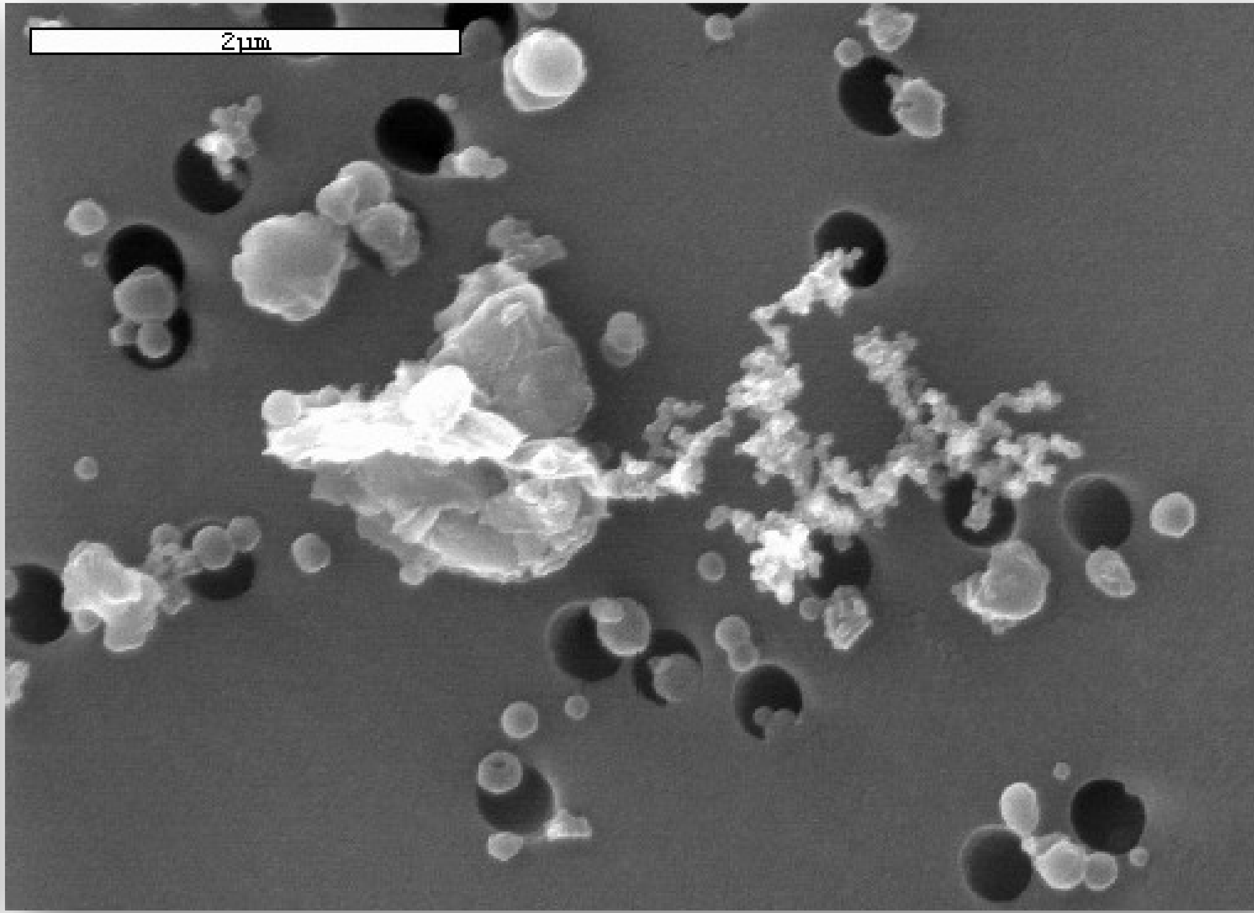

AMMA (2006), unpublished

The variability issue (3/3)

Complex refractive index (CRI) = n-ik

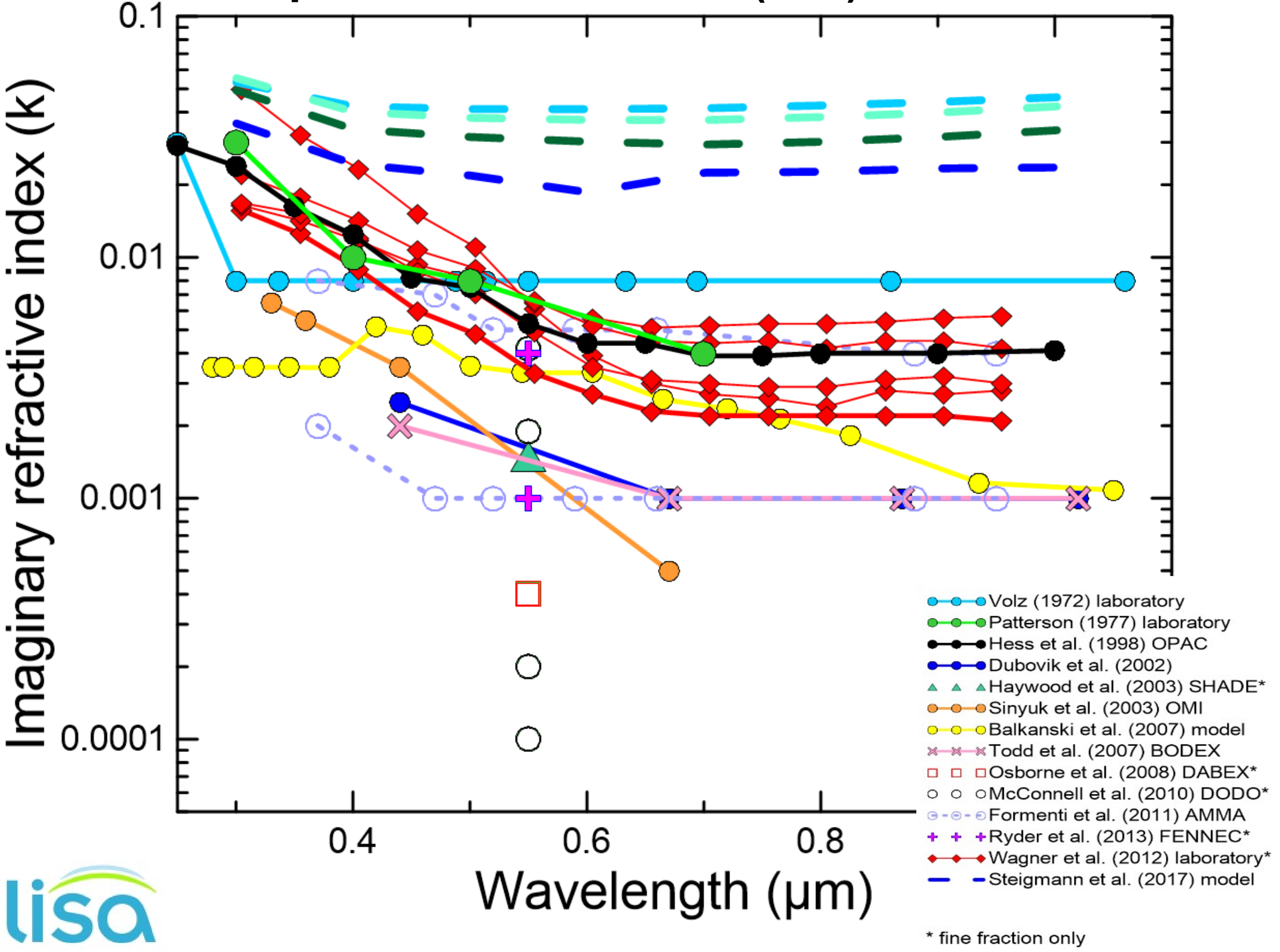

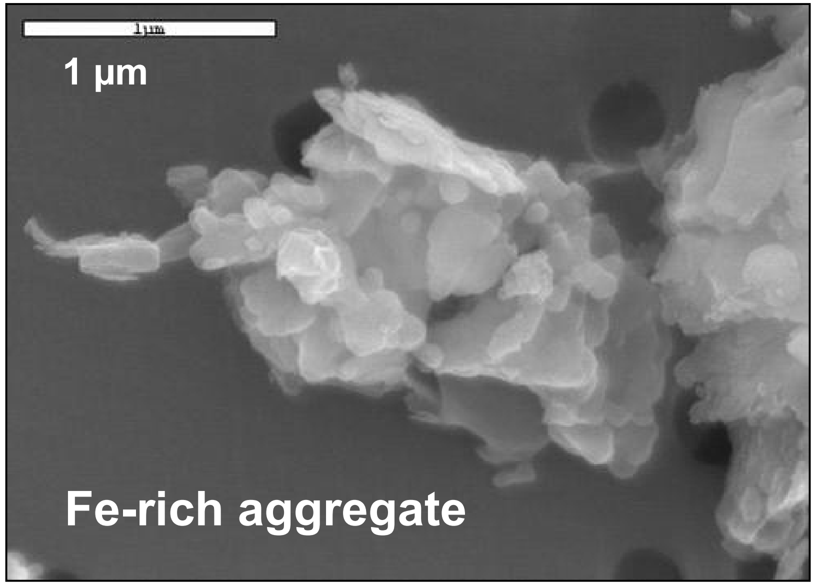

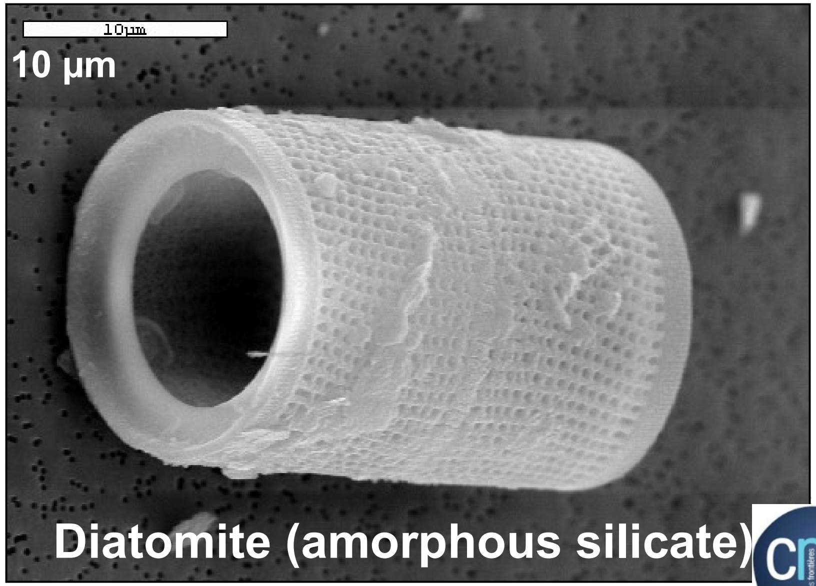

Advancing the prediction of optical properties and links to mineralogy

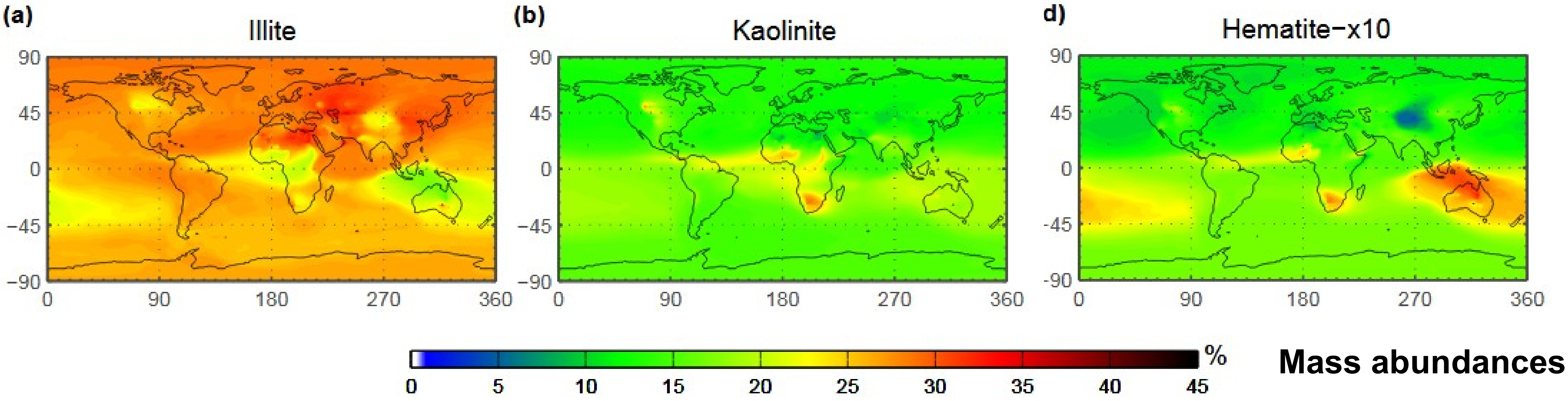

Mass abundances

Scanza et al., ACP, 2014
but also Colarco et al., JGR, 2014; Journet et al., ACP, 2014; Perlwitz et al, ACP, 2015a; 2015b

Approaches

Aircraft

Laboratory simulation

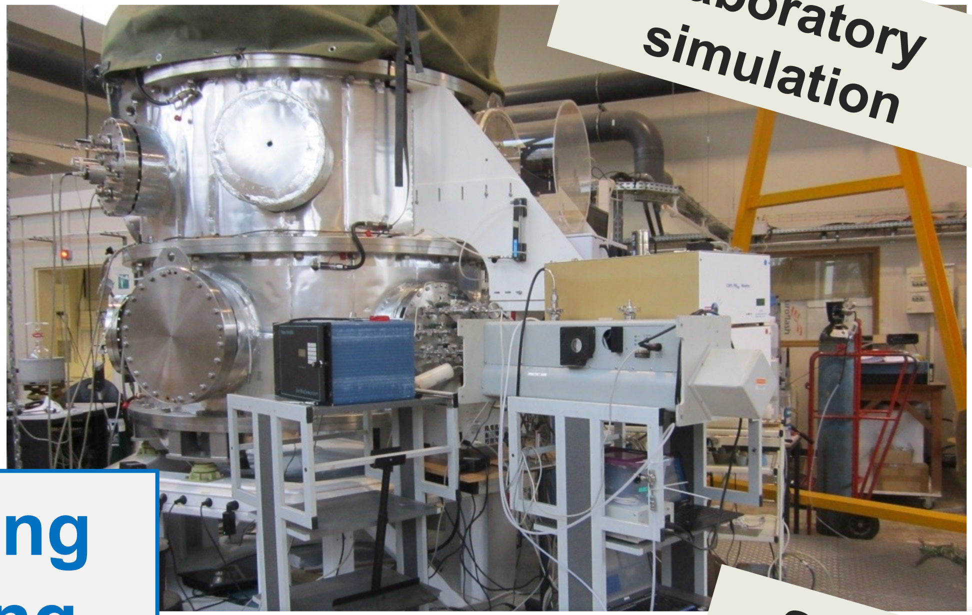

Understanding
Parametrising

Ground-based

Space

Approaches

Aircraft

Laboratory simulation

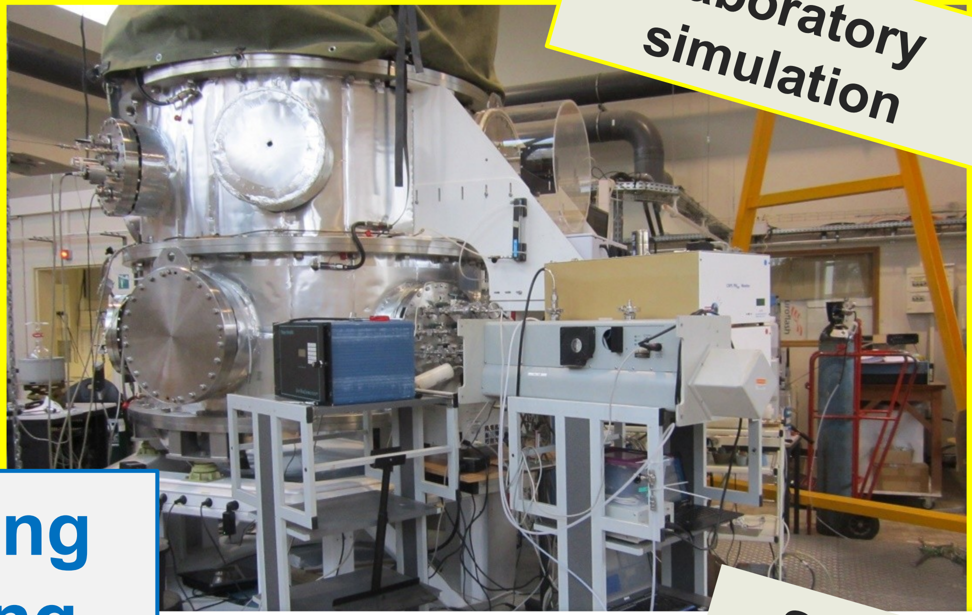

Understanding
Parametrising

Ground-based

Space

The CESAM simulation chamber

- Controlled conditions (RH, T, irradiation, gaz mixtures)
- Simultaneous measurements of physico-chemical and optical properties
- Long aerosol lifetime (> 24h for submicron particles)

Stainless-steel, 4.2 m^3 volume

Wang et al., AMT, 2011

A number of challenges

Generating mineral dust aerosols from natural soils

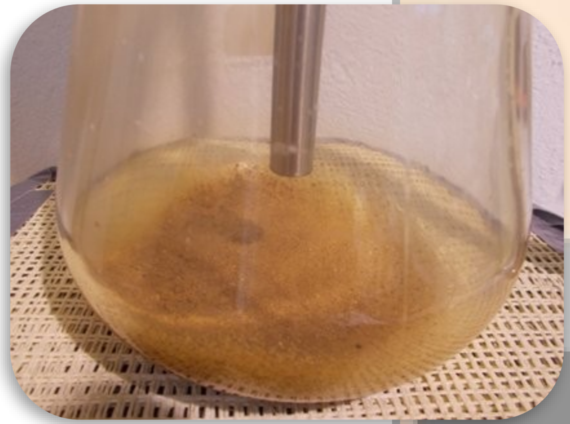

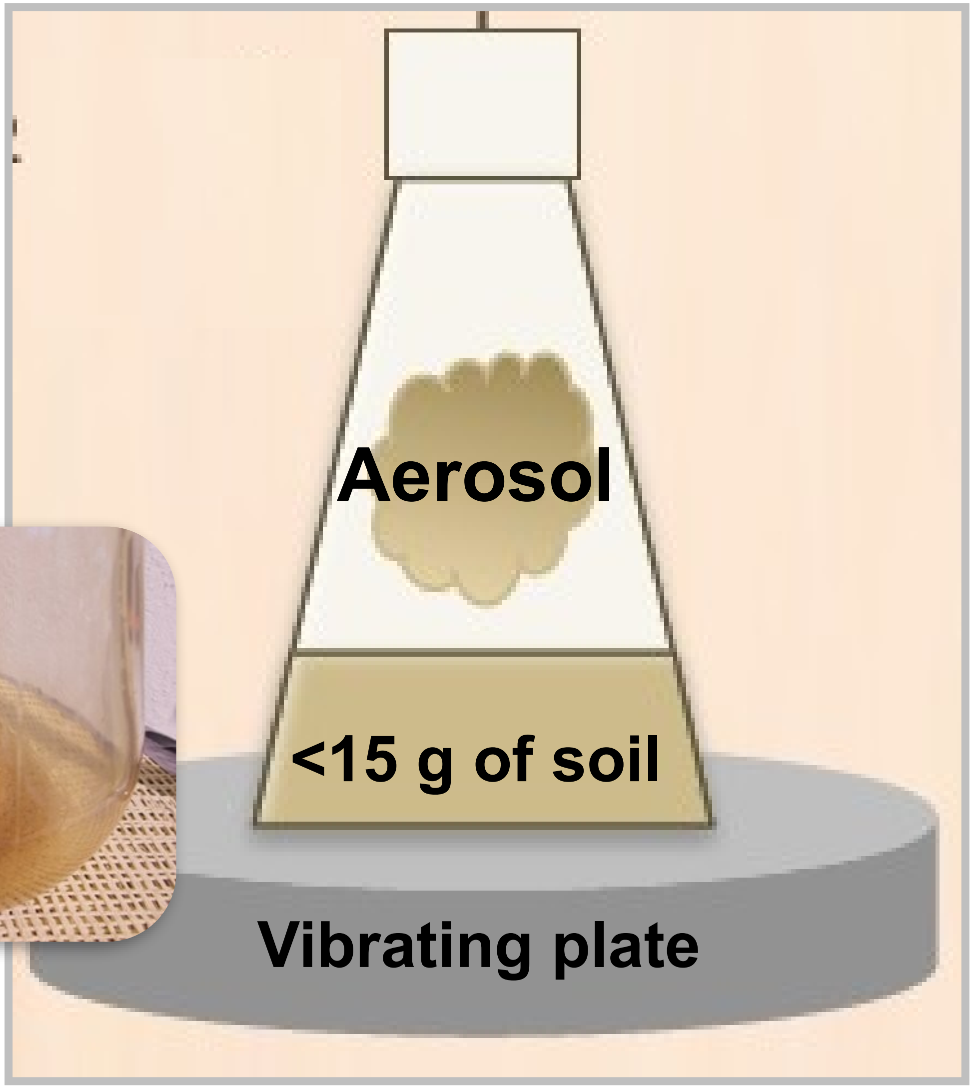

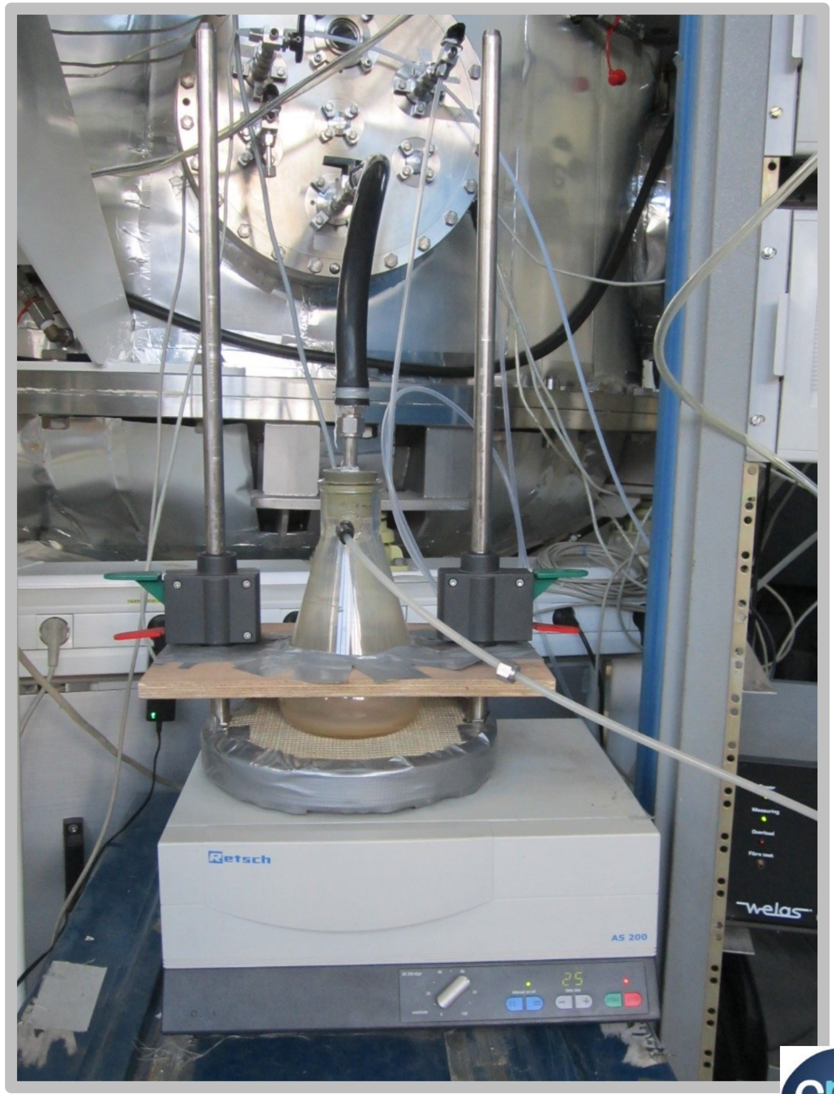

It seem to works…

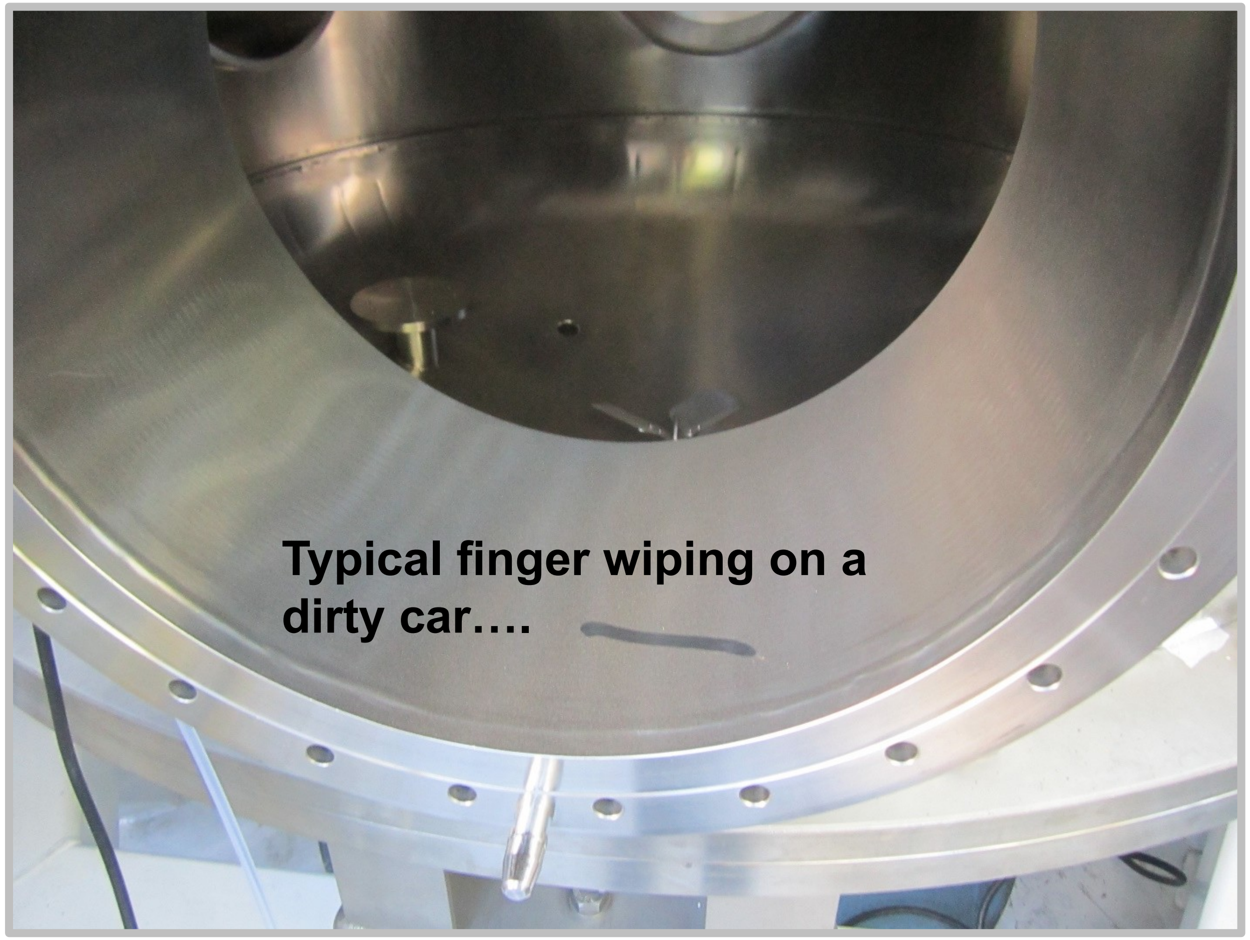

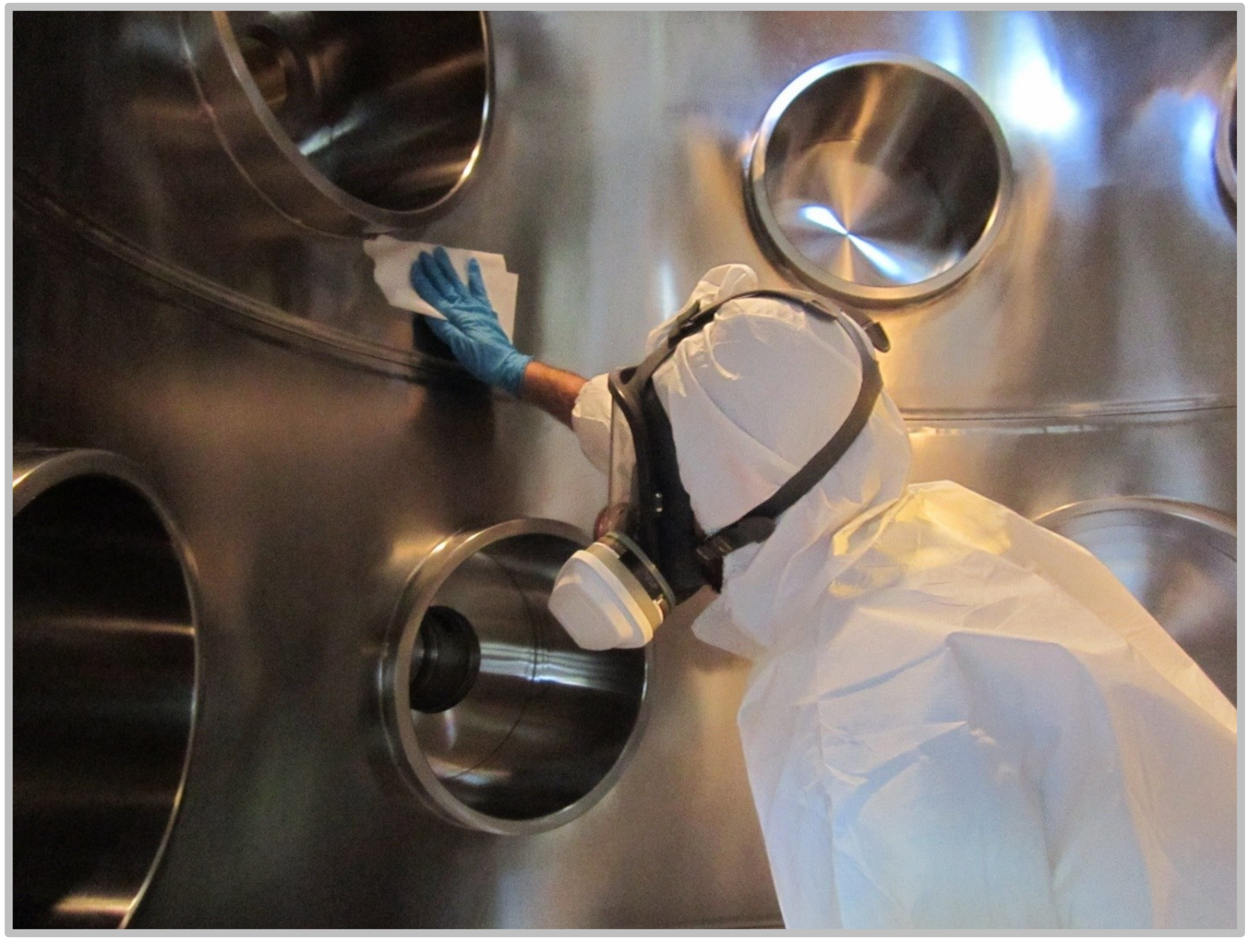

Particle lifetime and concentration

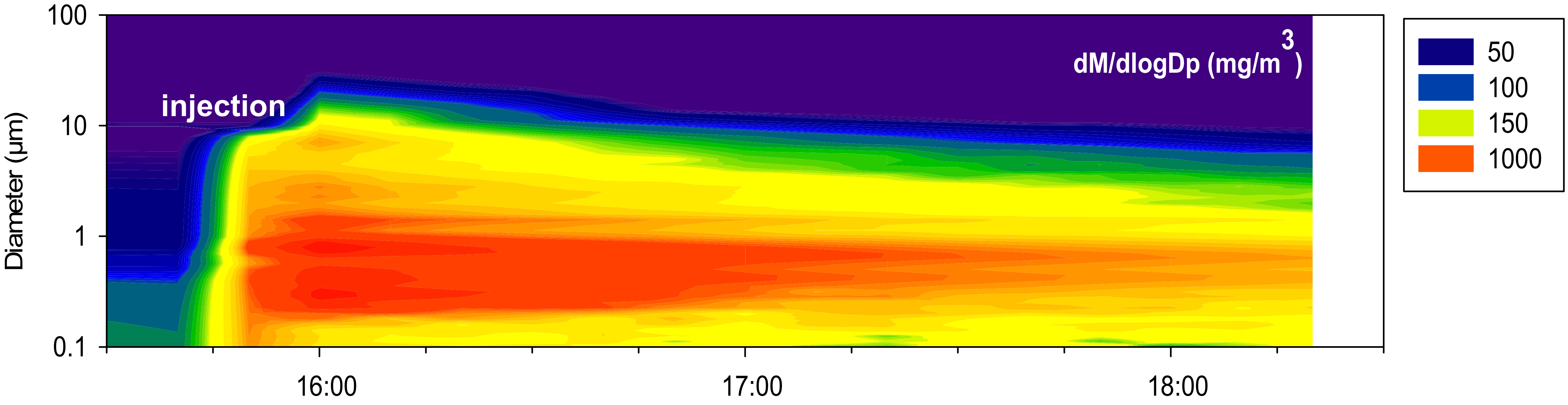

Dust aerosols everywhere, at the same concentration….

GRIMM OPC
0.26-31 µm

GRIMM OPC
0.26-31 µm

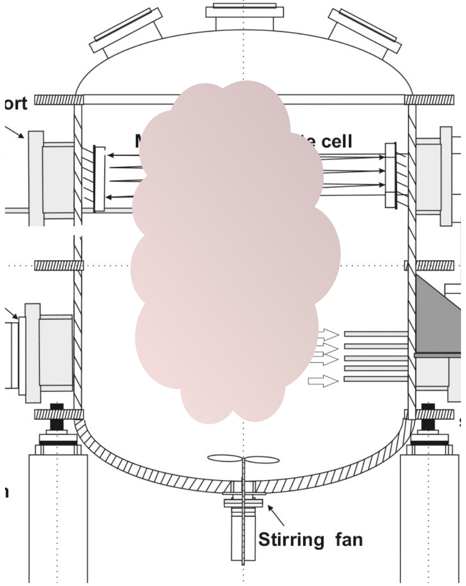

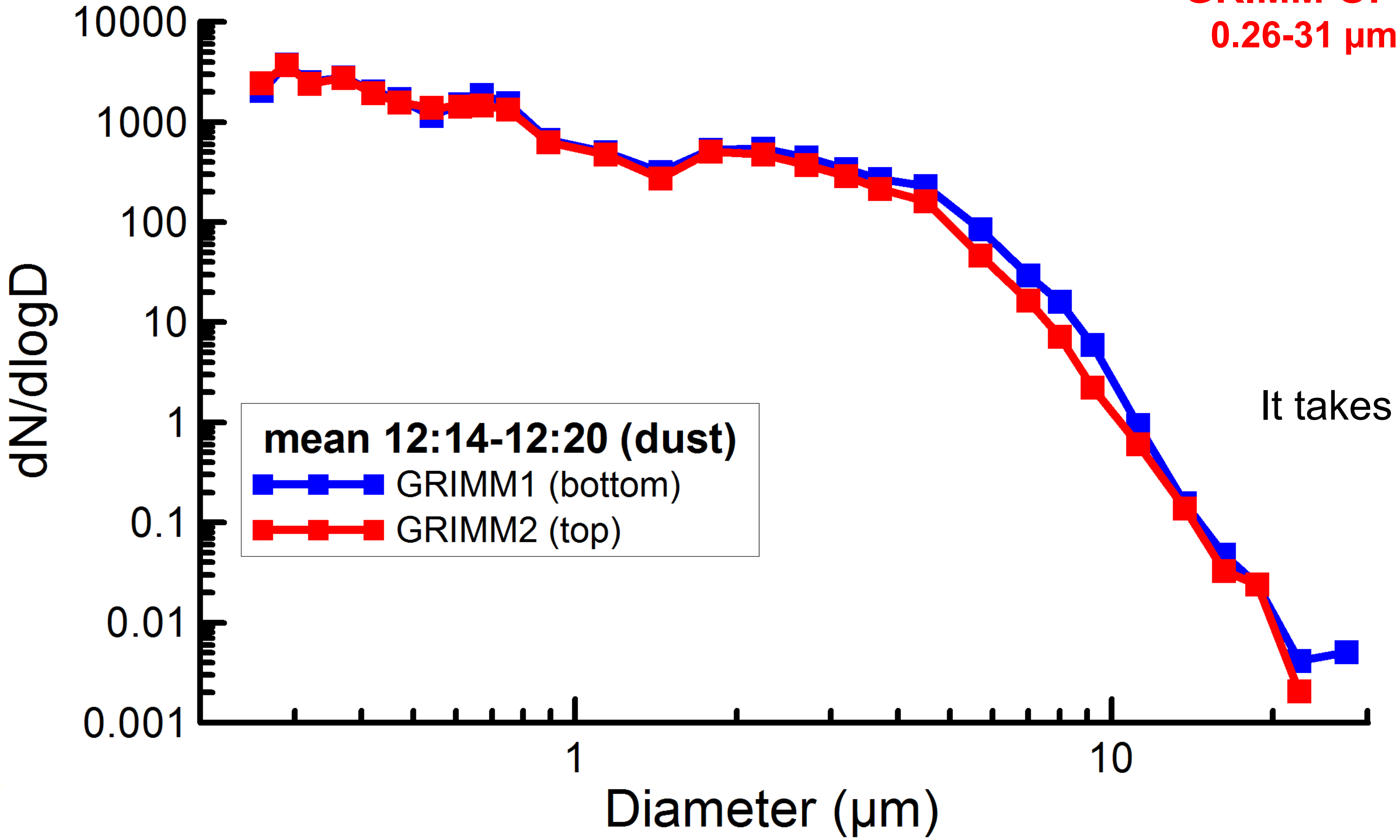

It takes about 15 mins after injection

Size-dependent dust aerosol lifetime

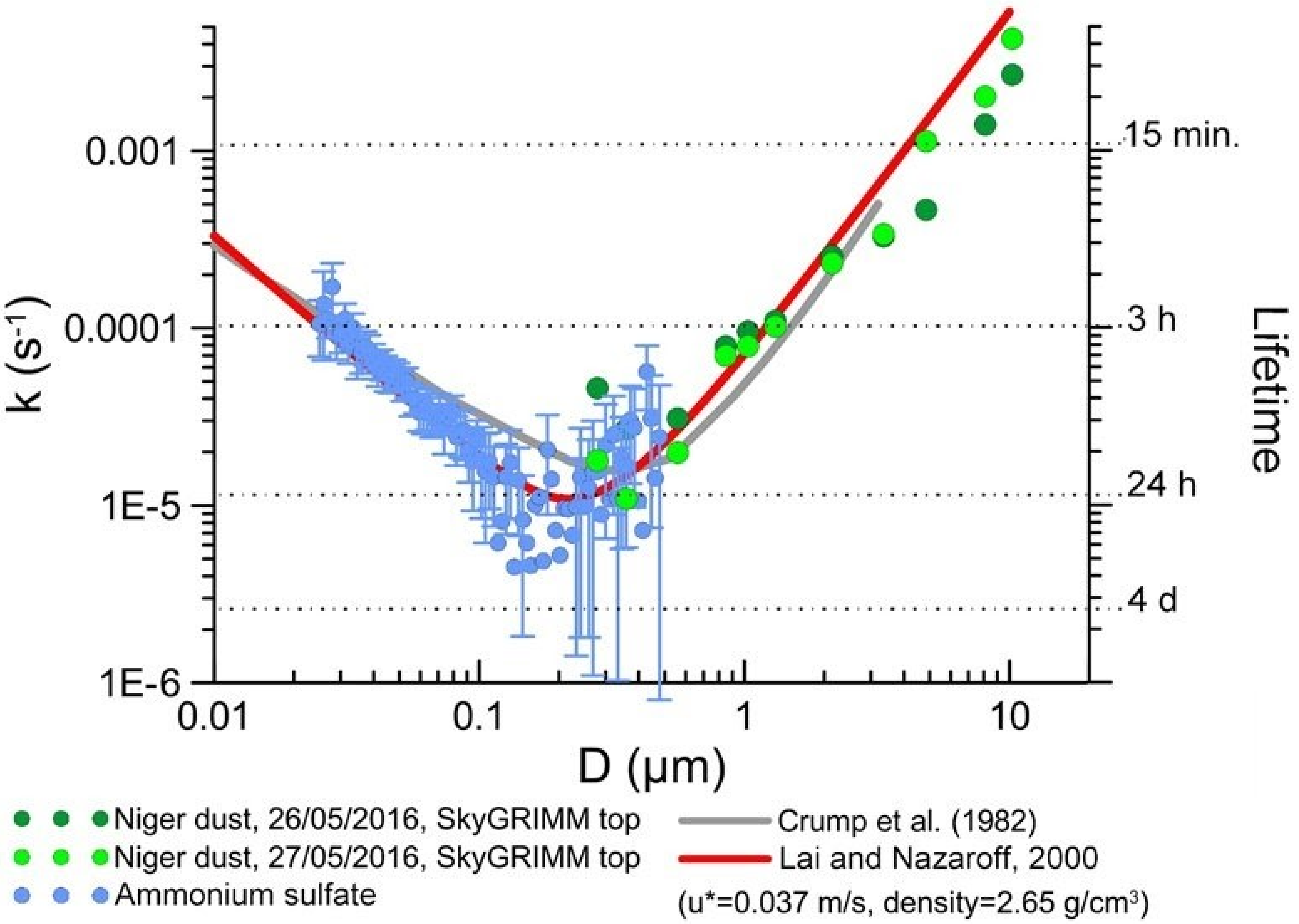

SMPS
0.019-0.8 µm

GRIMM OPC
0.26-31 µm

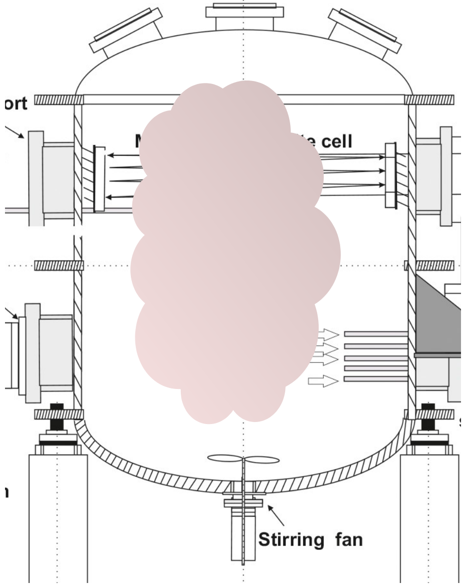

Quantifying the dust aerosol mineralogy

Total mass = Mass of crystalline minerals + Mass of iron oxydes + Mass of amorphous material

Total mass = gravimetrically or by elemental analysis (XRF, PIXE) or by conversion of particle size distribution
Mass of crystalline minerals = X-ray diffraction (XRD)
Mass of iron oxydes = X-ray absorption at near-edge spectroscopy (XANES)
Mass of amorphous material = TEM counting of non-diffracting particles

Clay (aluminosilicate)

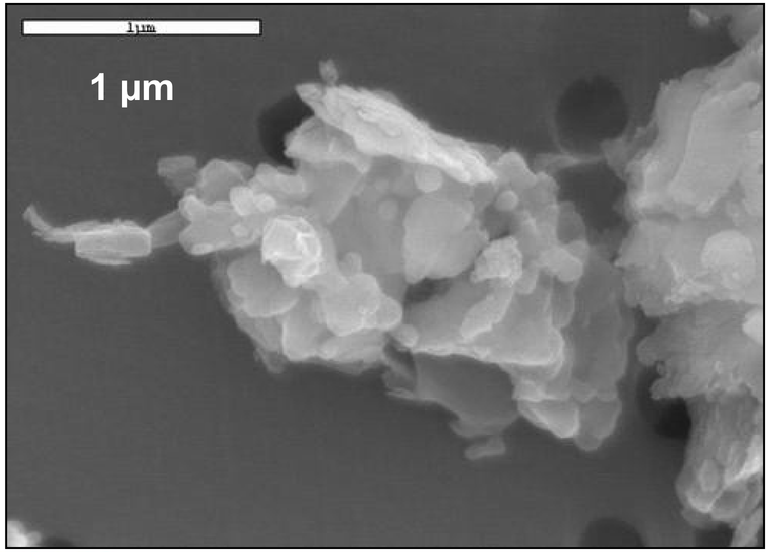

Gypsum (calcium sulphate)

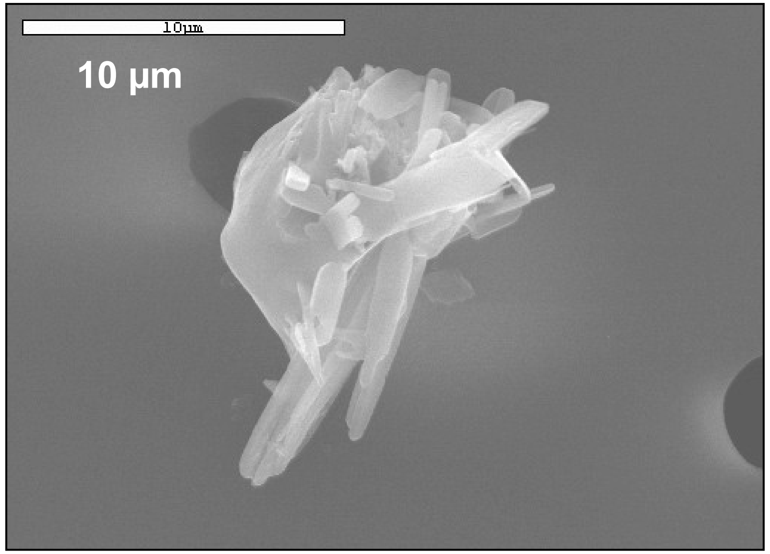

Diatomite (amorphous silicate)

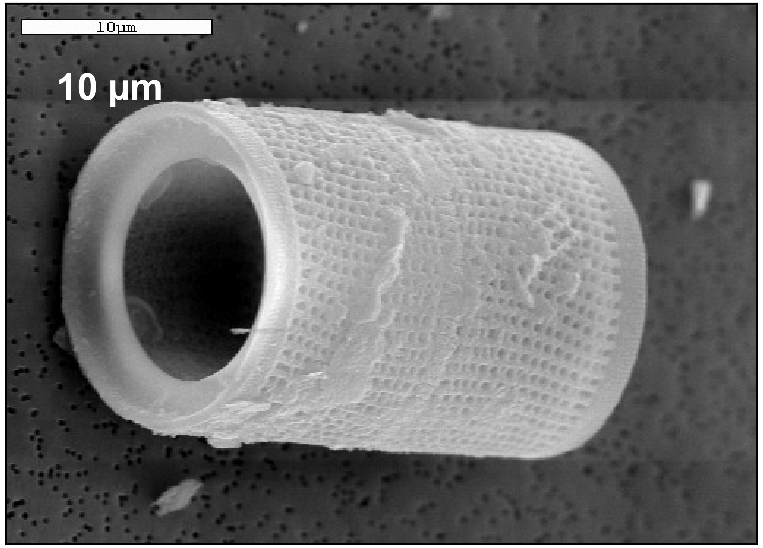

Quantifying the dust aerosol mineralogy

Mass of crystalline minerals = X-ray diffraction (XRD)

Identification

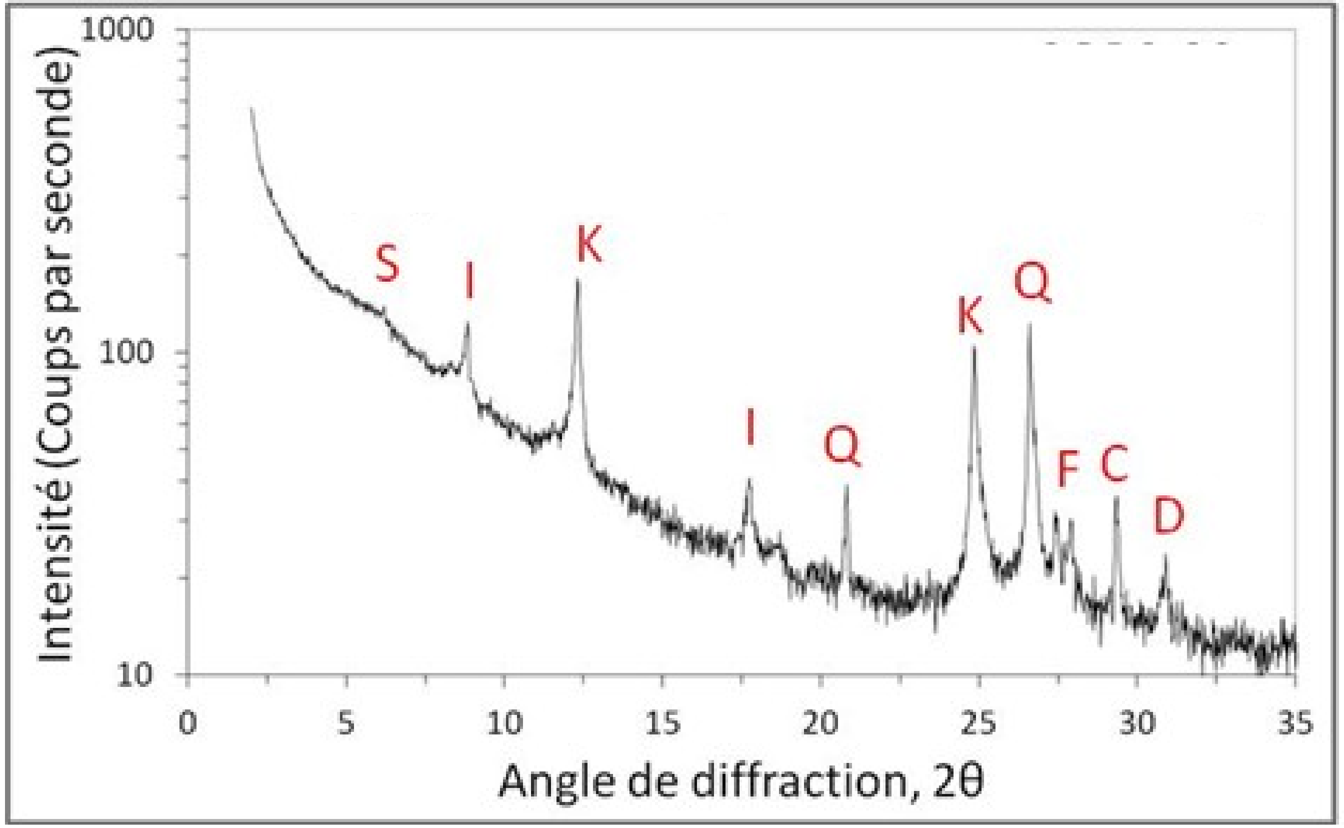

XRD analysis of low-mass samples (< 600 µg)
Caquineau et al. (1997)

Quantification

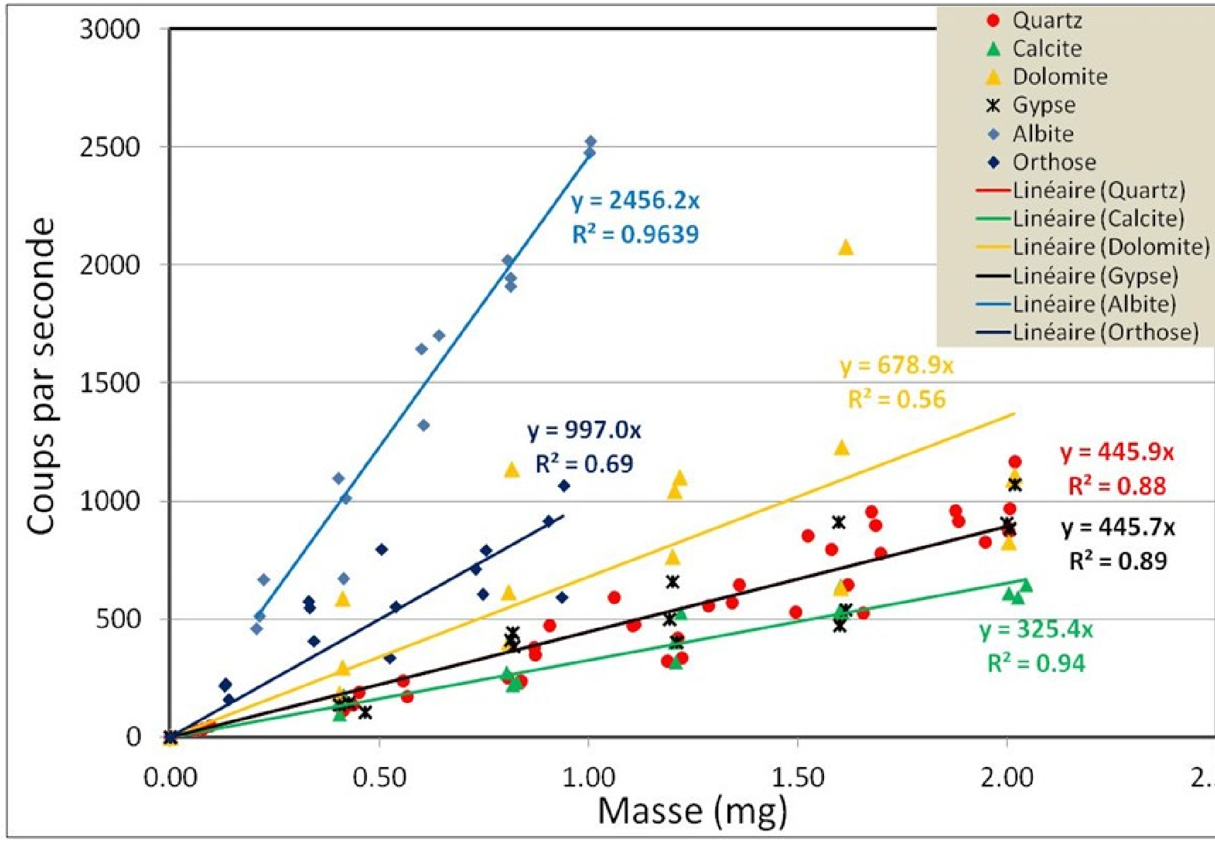

Calibration of non-clay minerals (Klaver et al., 2011)
Clay minerals based on difference with total mass

Quantifying the dust aerosol mineralogy

Fe absorption edge **First derivative**

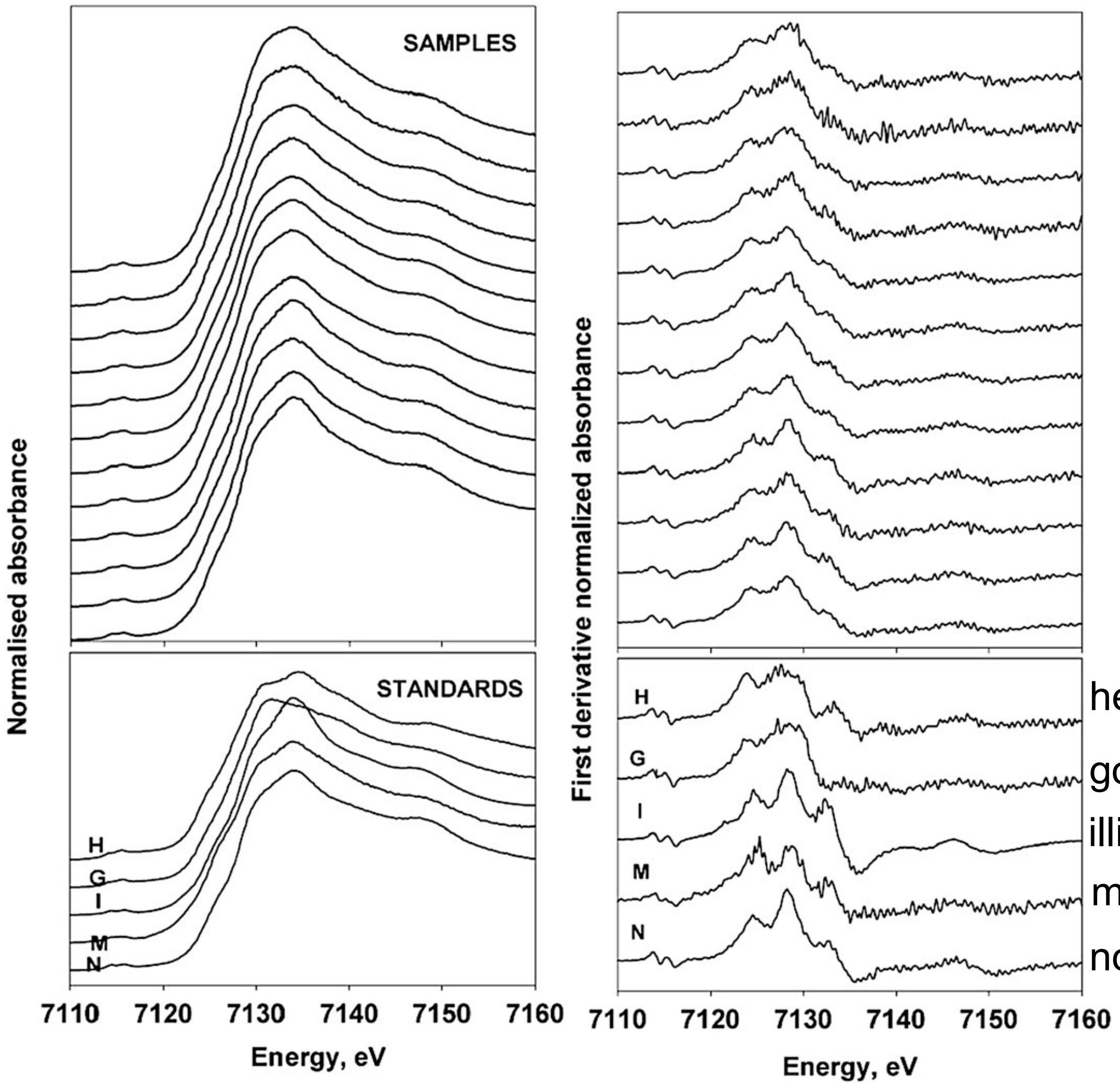

hema
goetl
illite
montmorillonite
nontronite

Mass of iron oxydes = X-ray absorption at near-edge spectroscopy (XANES)

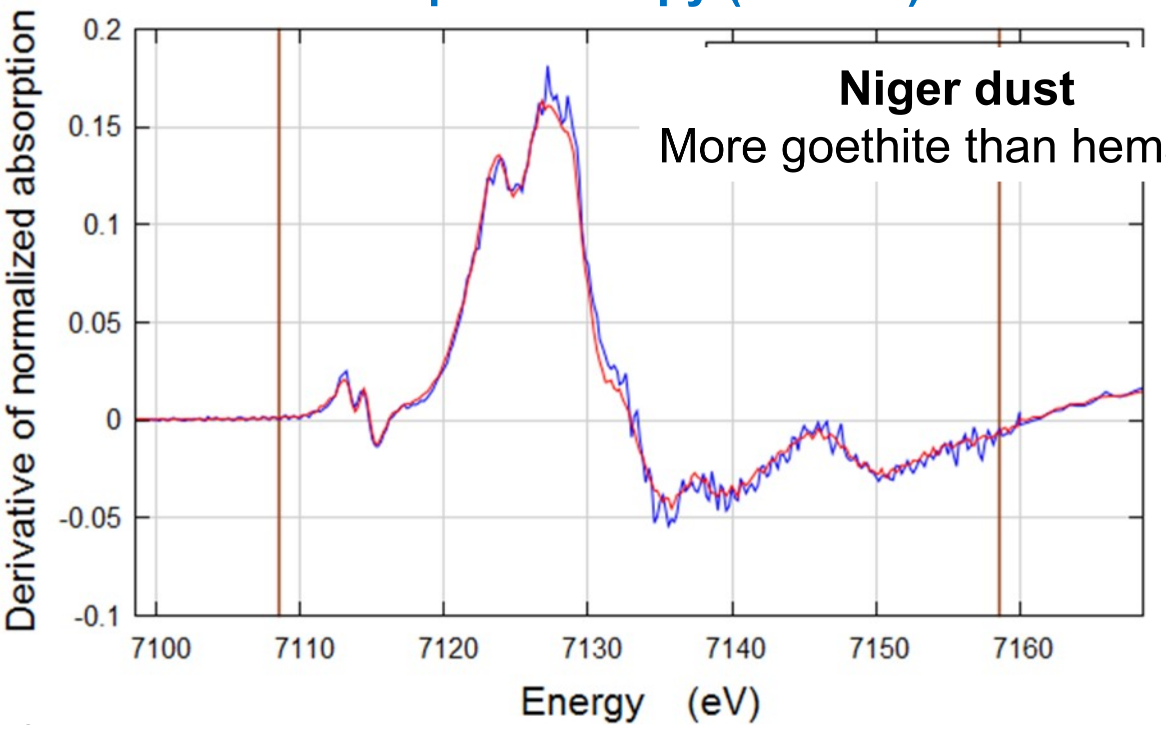

Formenti et al. (2014)

Realism of the generated aerosol

Size distribution

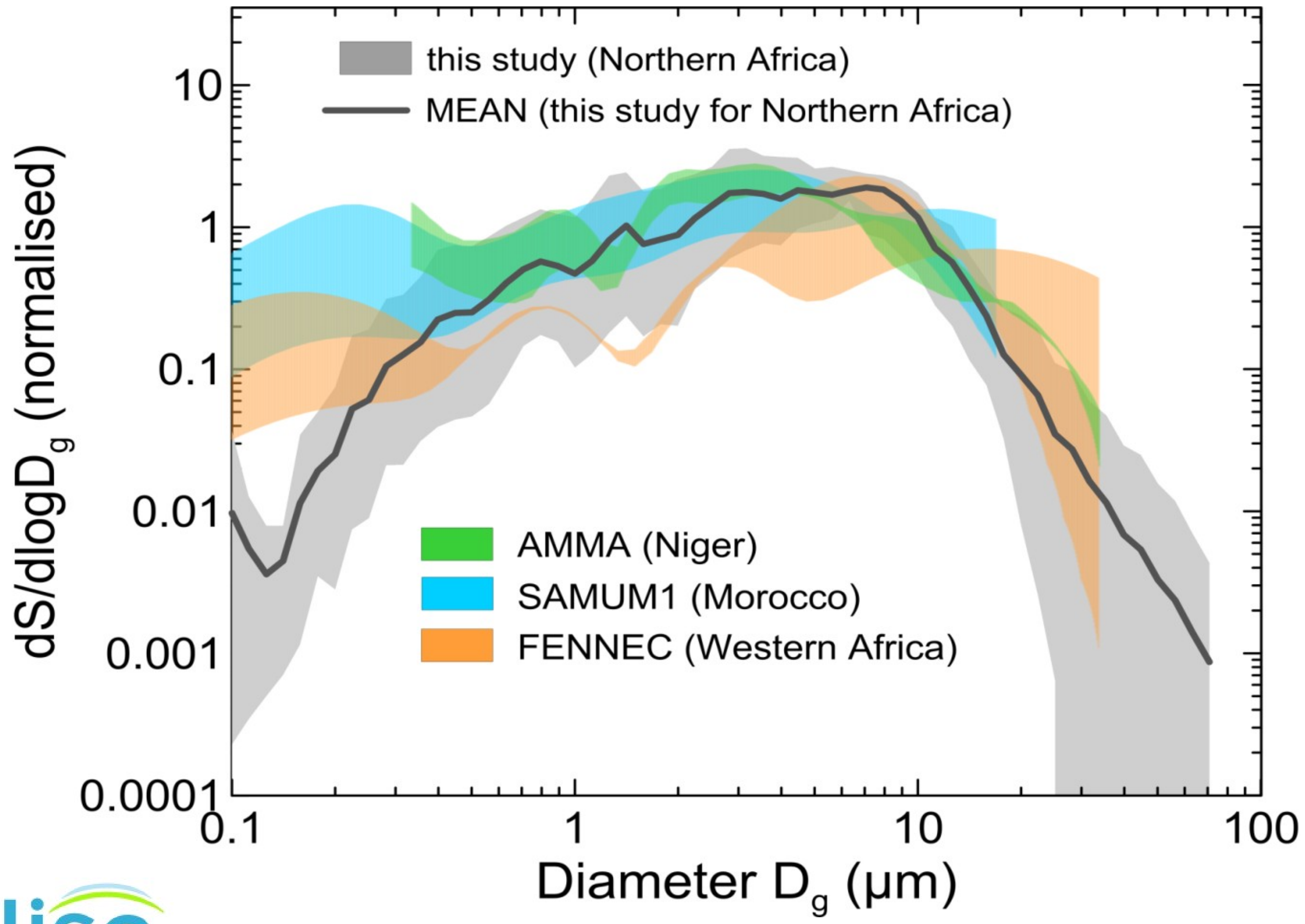

Mineralogy

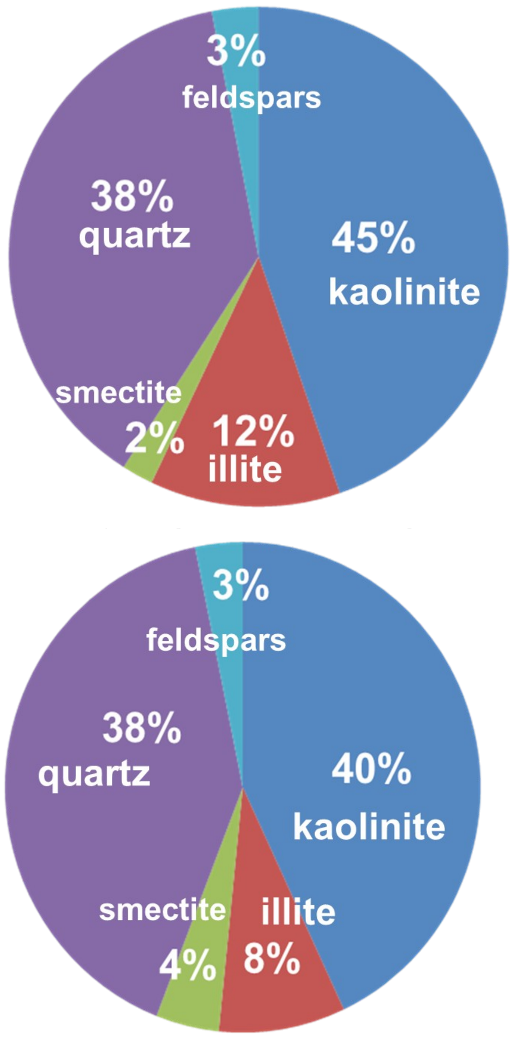

Niger dust CESAM

Niger dust in the field

RED-DUST

A laboratory-based project
targeting the absorption properties of mineral dust

wavelength
soil mineralogy
size distribution

Laboratory simulation experiments

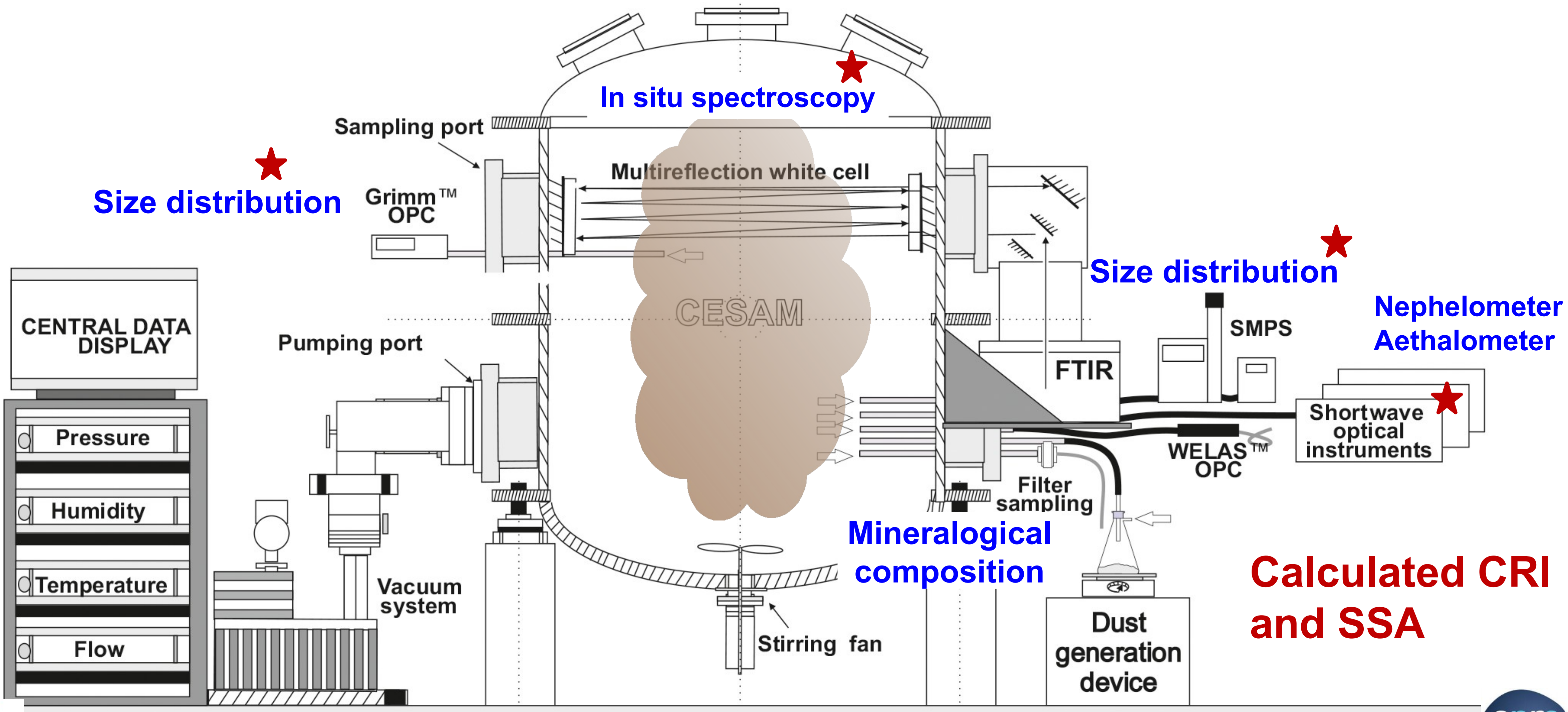

Representation of the global soil mineralogical composition

Goethite

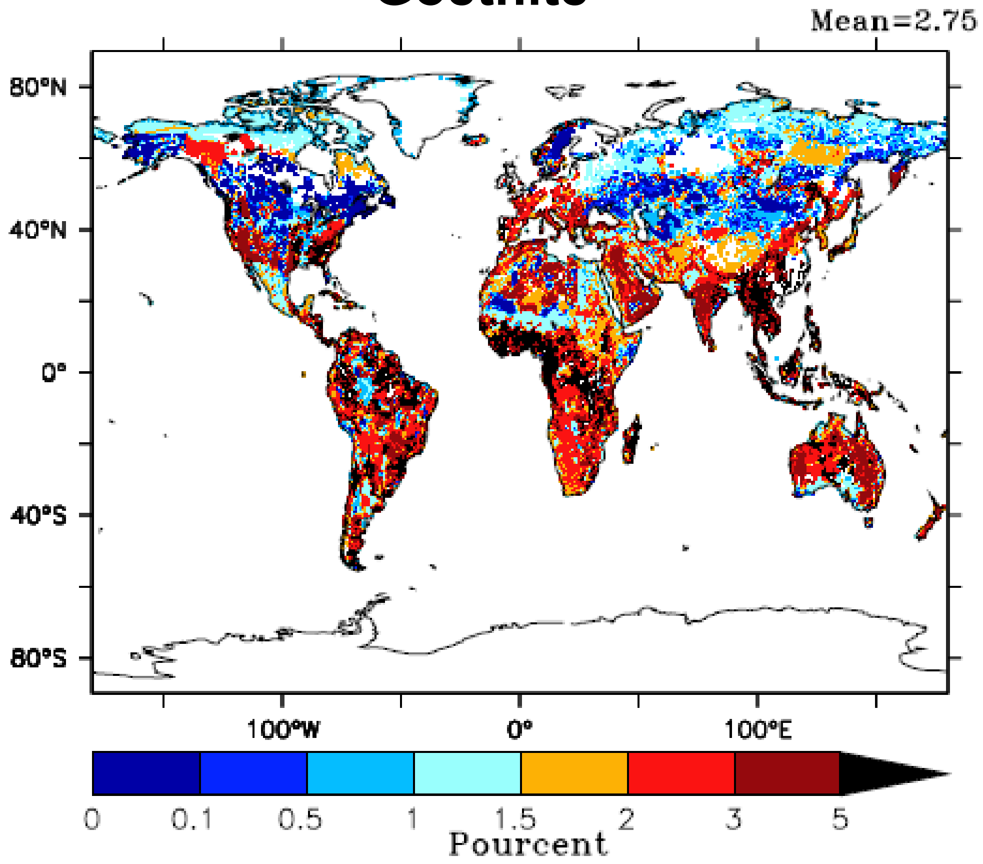

Hematite

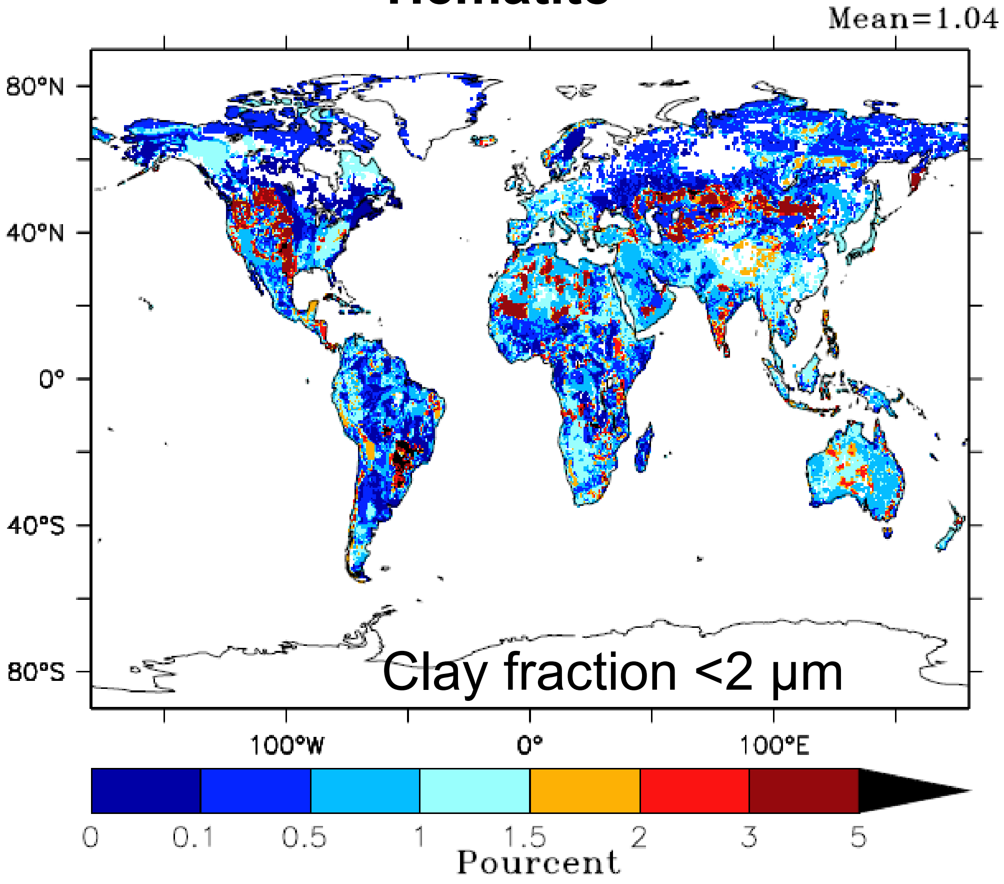

Soil mineralogical database, Journet et al. (2014)

Selected soils for experiments

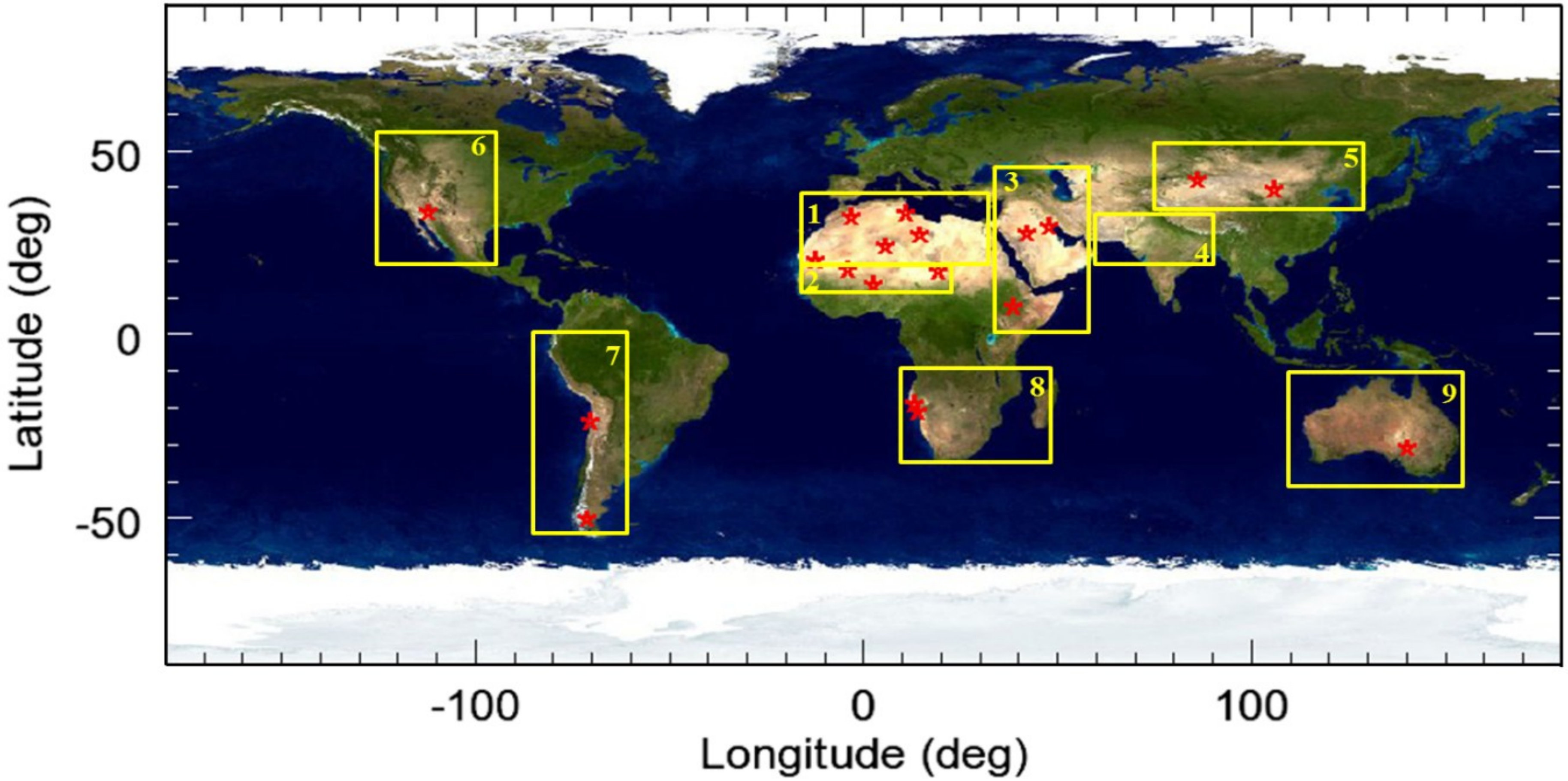

Yellow rectangles: desert areas by Ginoux et al. (2012)

RED-DUST

Choice of samples from soil bank

Relevant to UV/VIS | Relevant to IR

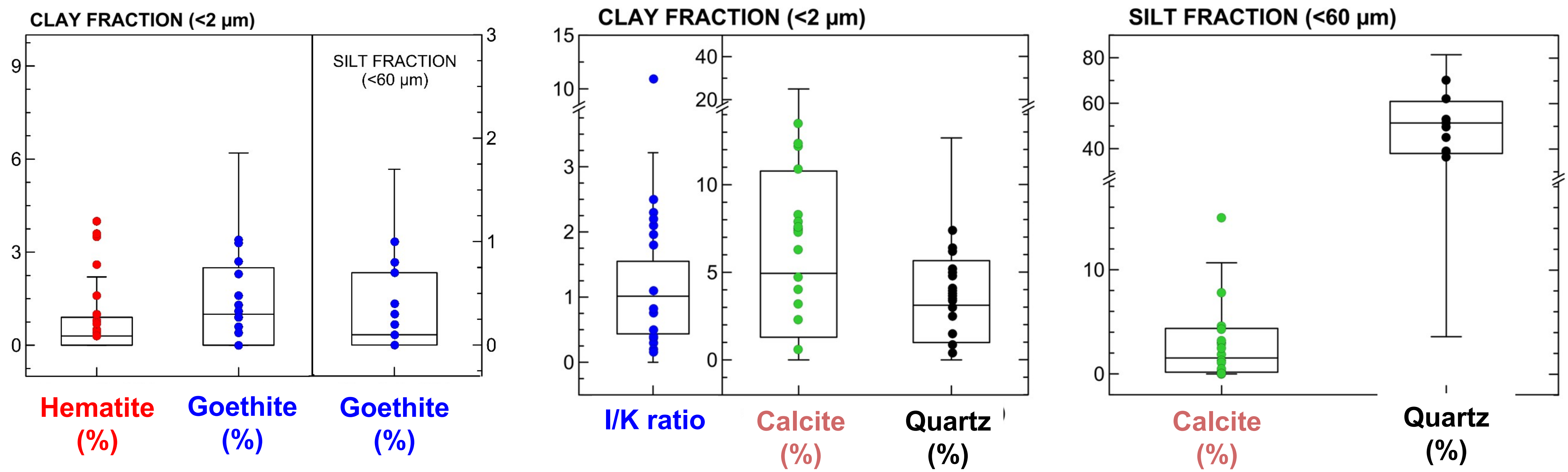

Dots = selected soils
Box and Whiskers = global soils (Journet et al., 2014)

Soil and aerosol mineralogy

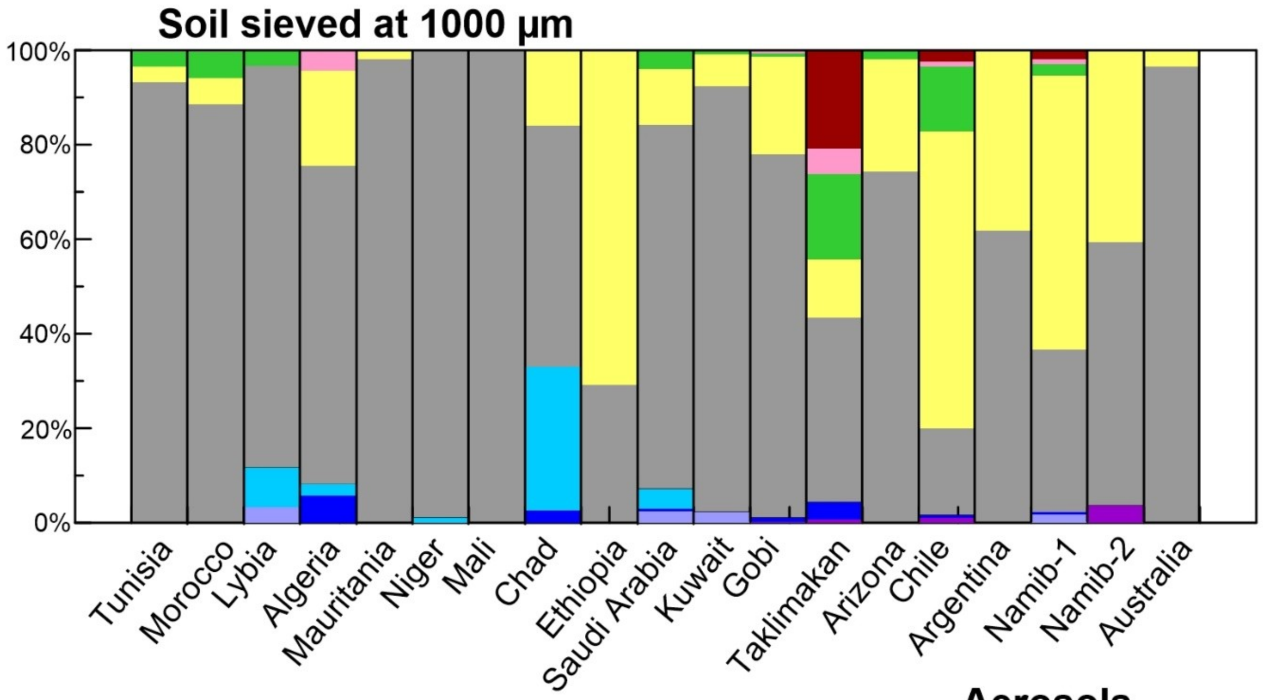

+ Iron oxides < 7%

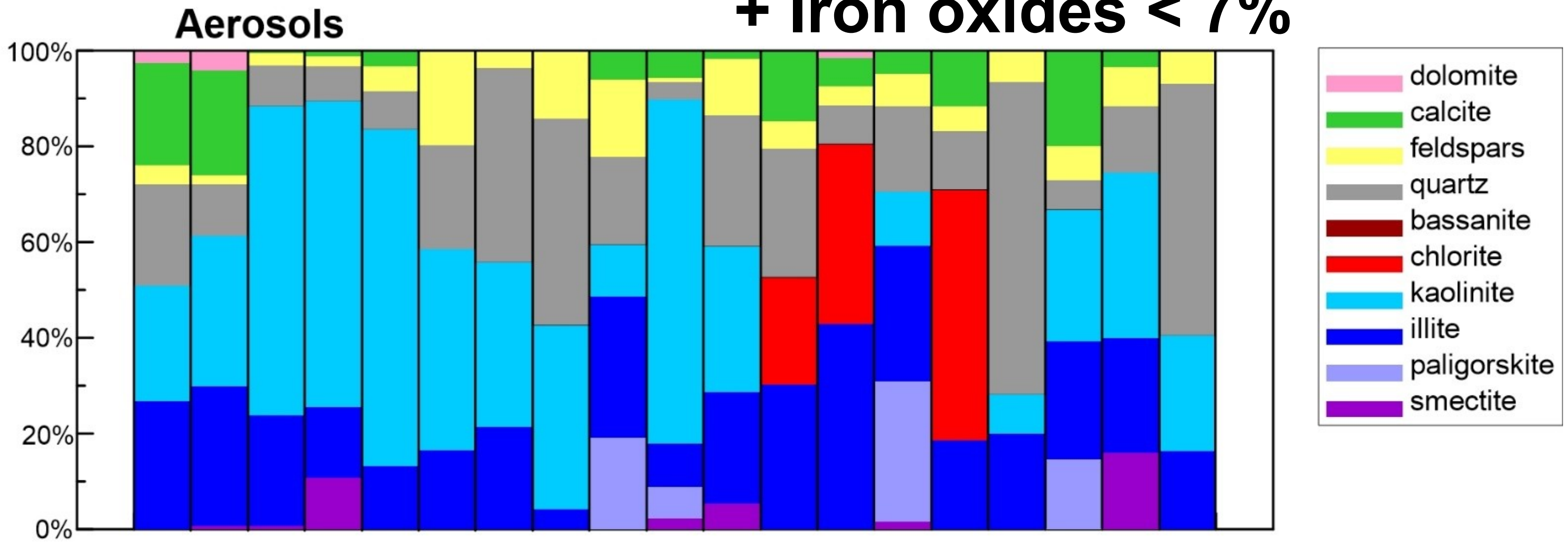

Representing the size distribution

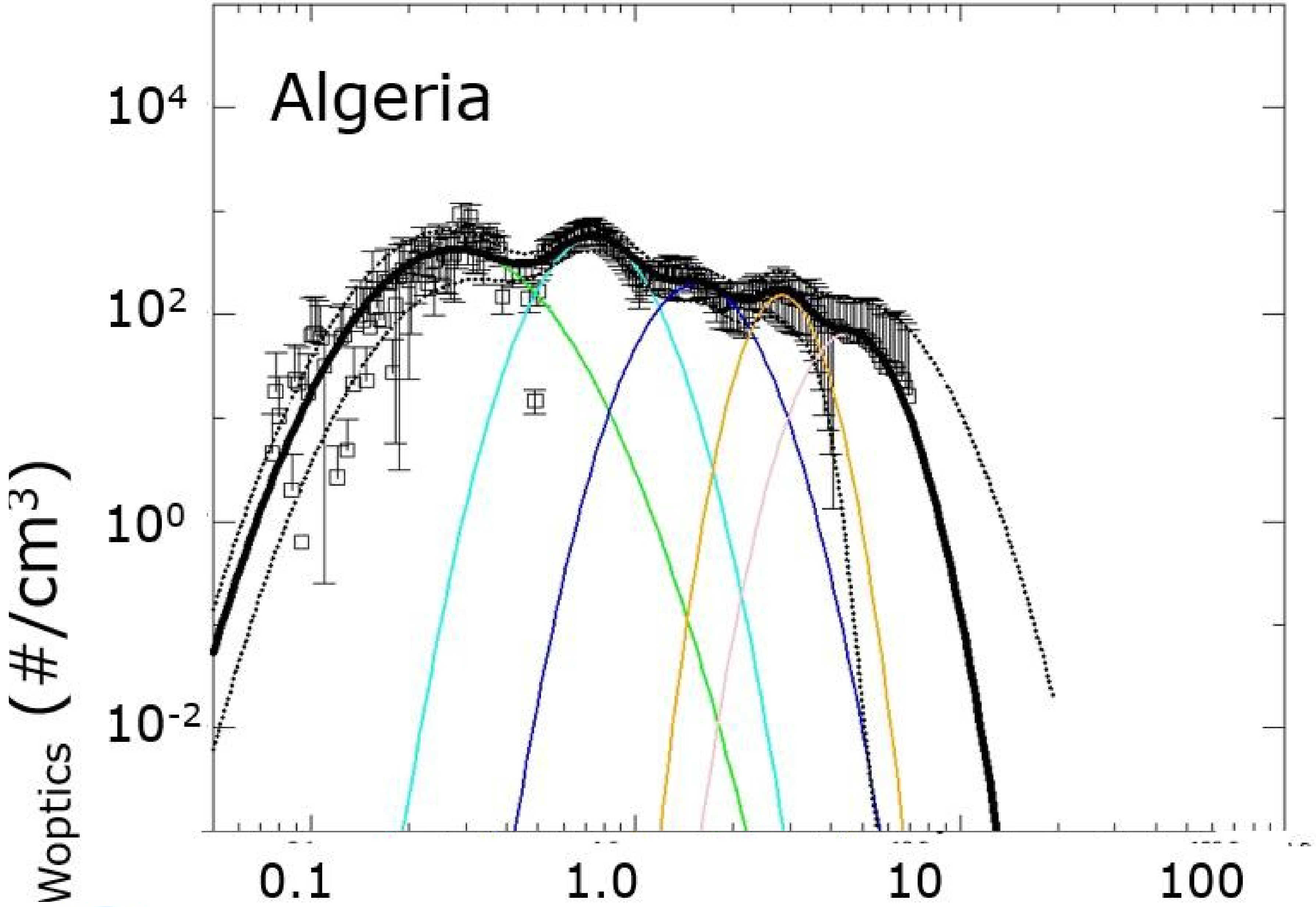

Modification of the IR spectrum

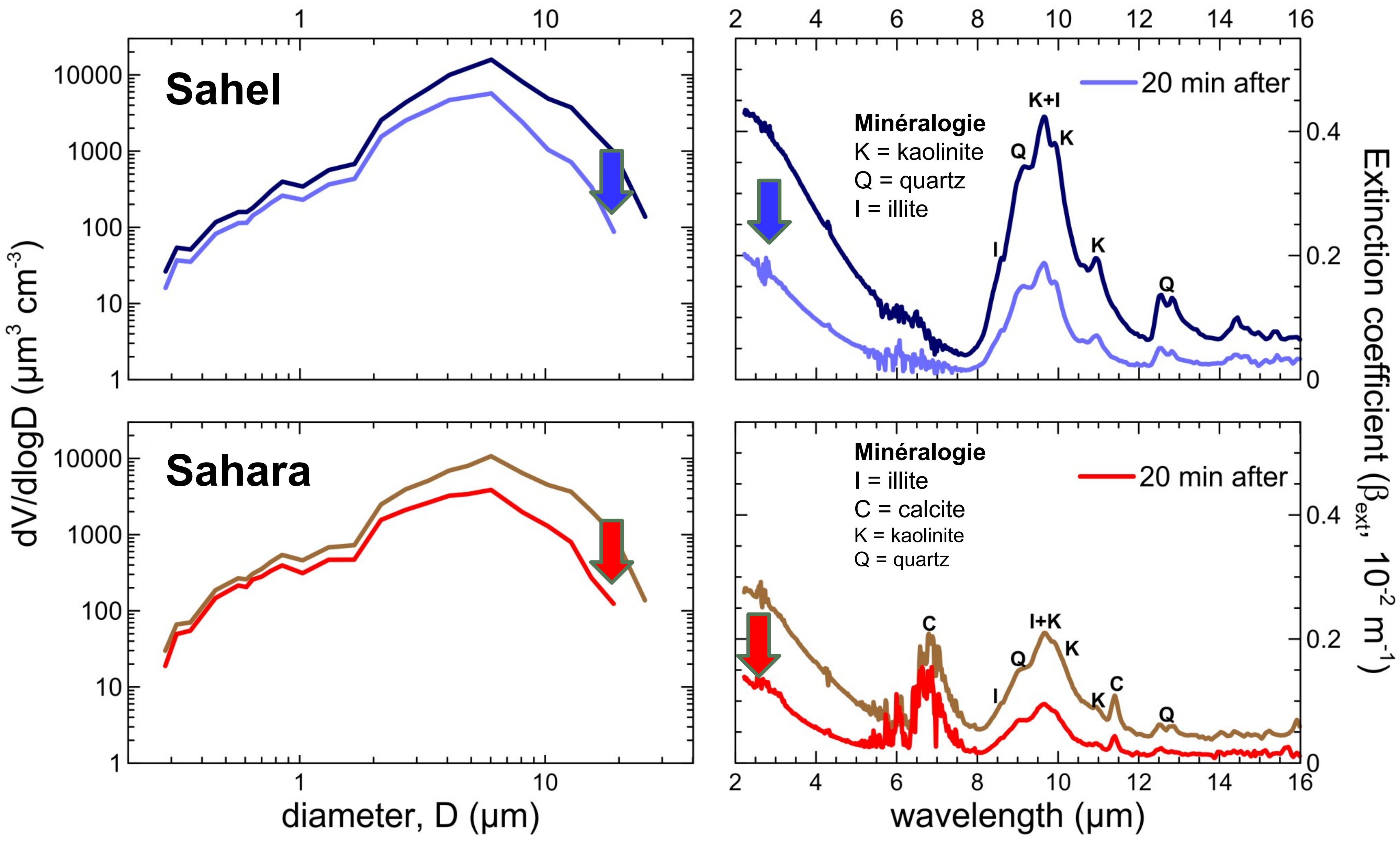

Complex refractive index: imaginary part

RED-DUST

UV/Vis

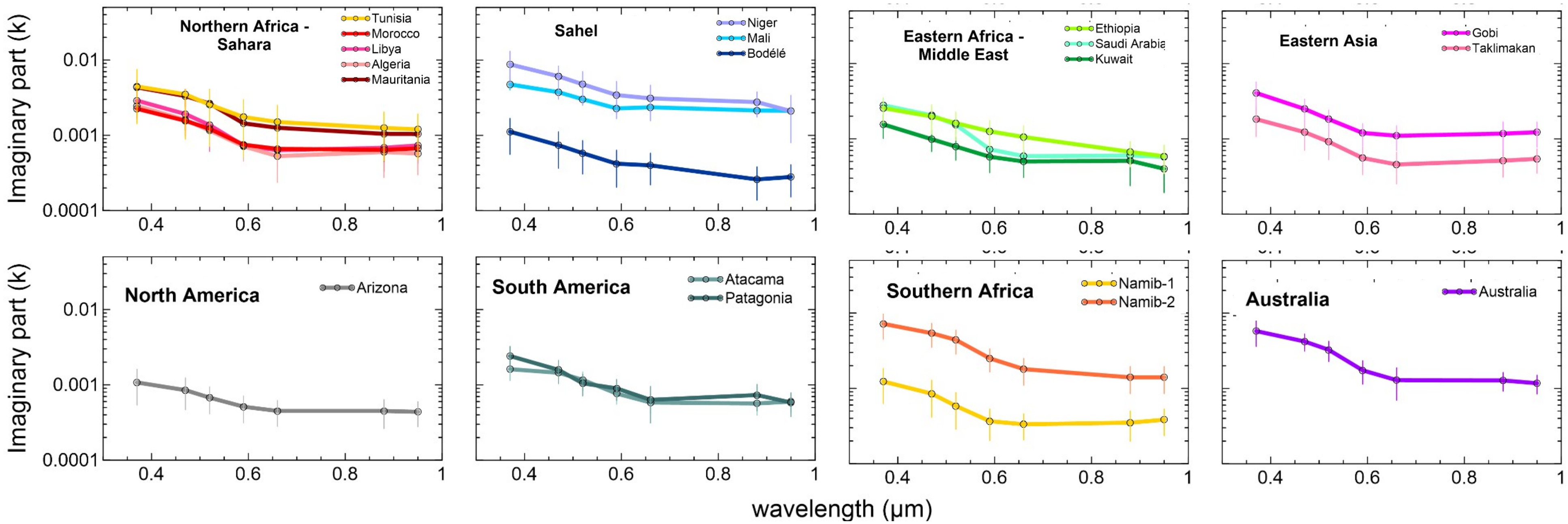

IR

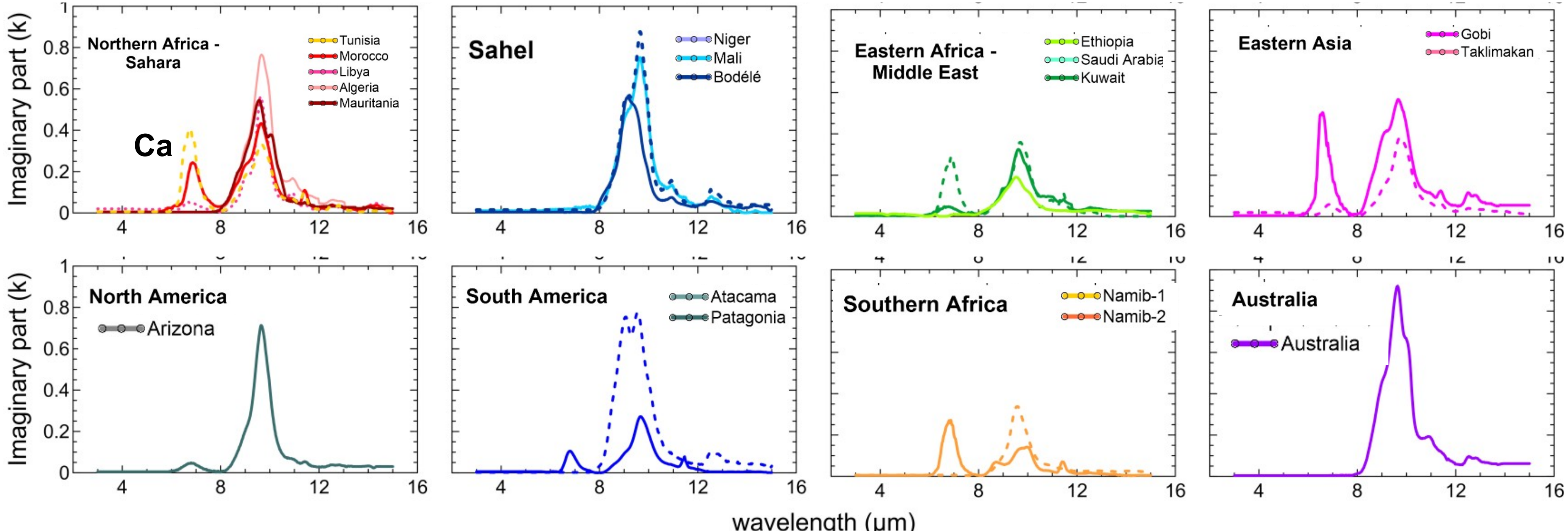

RED-DUST

Synthesis and comparison

UV/Vis

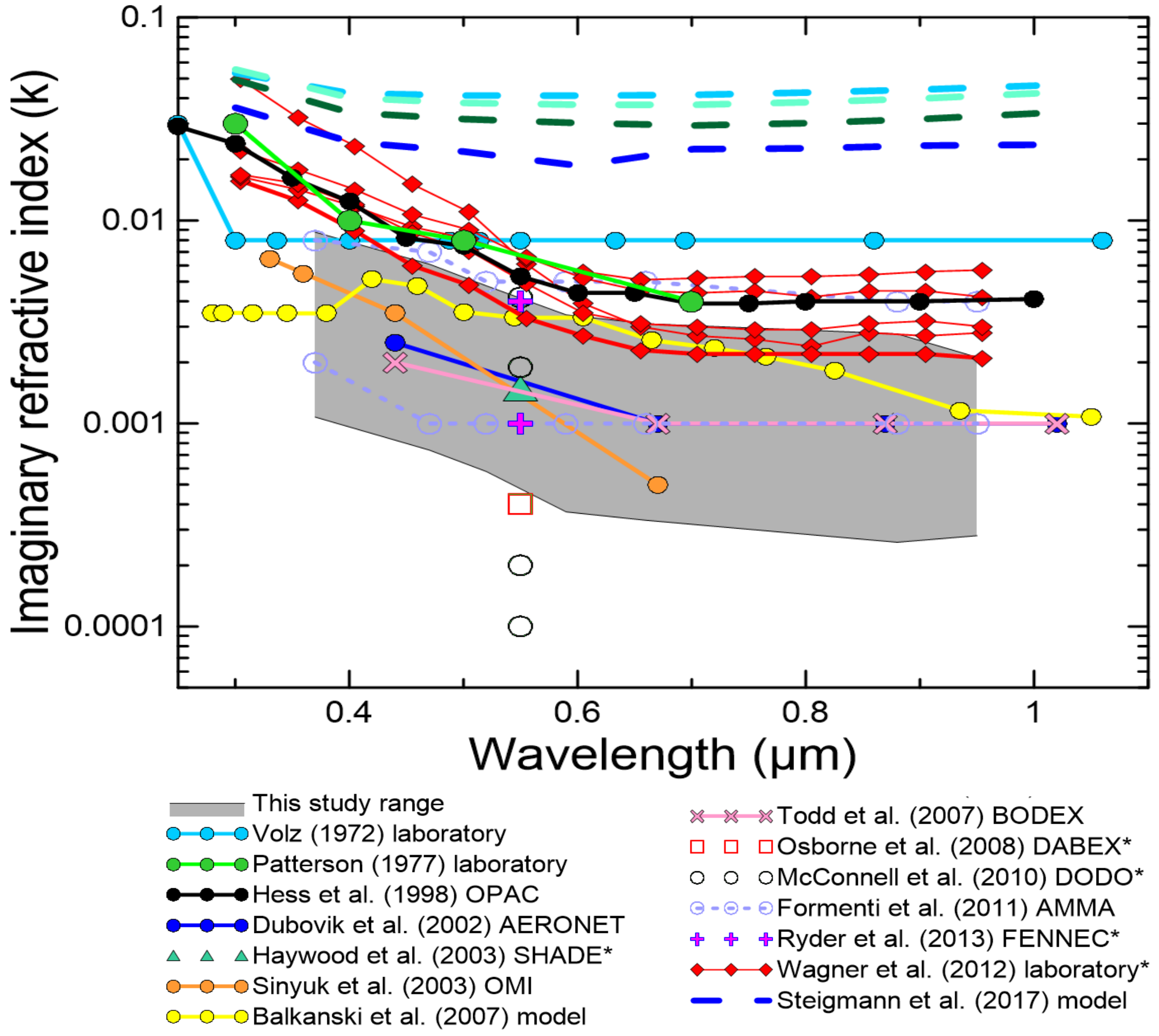

IR

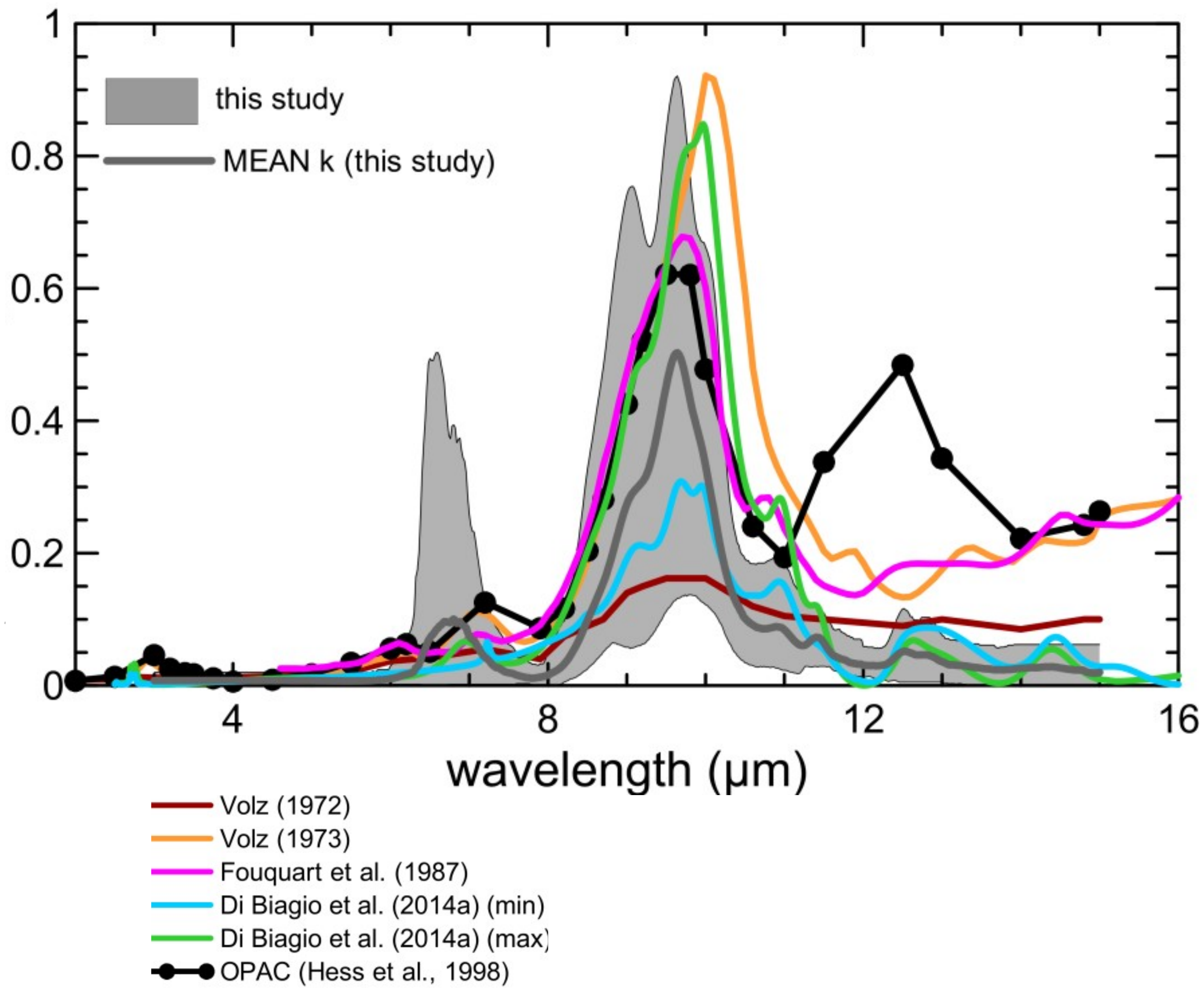

A relatively narrow range of values, little if no spectral dependence for the real part

Advancing the prediction of optical properties and links to mineralogy

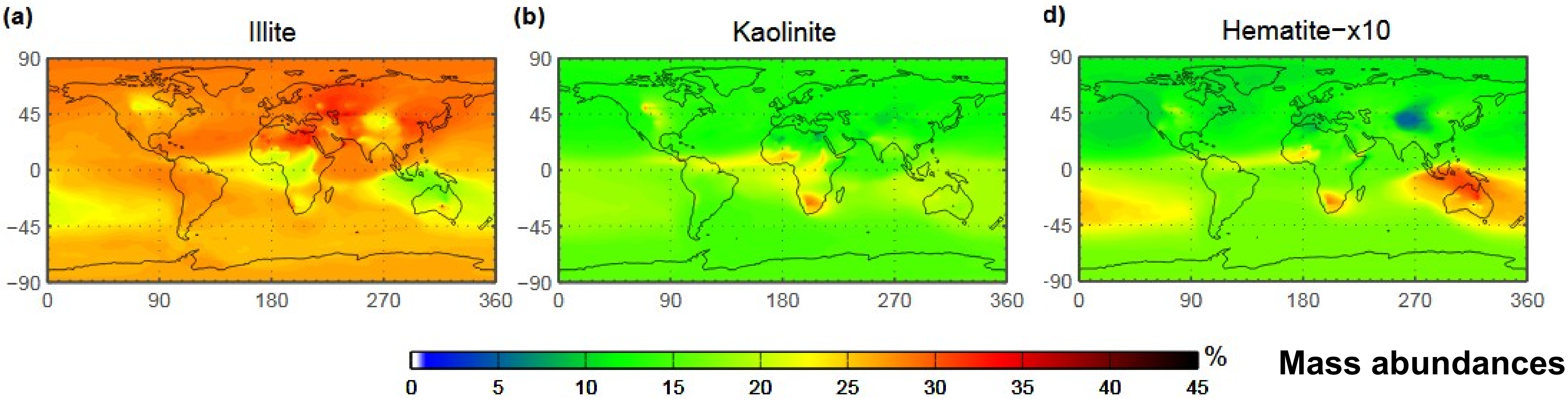

Mass abundances

Scanza et al., ACP, 2014
but also Colarco et al., JGR, 2014; Journet et al., ACP, 2014; Perlwitz et al, ACP, 2015a; 2015b

Imaginary CRI = f (mineral content) ?

UV/Vis CRI vs mineralogy

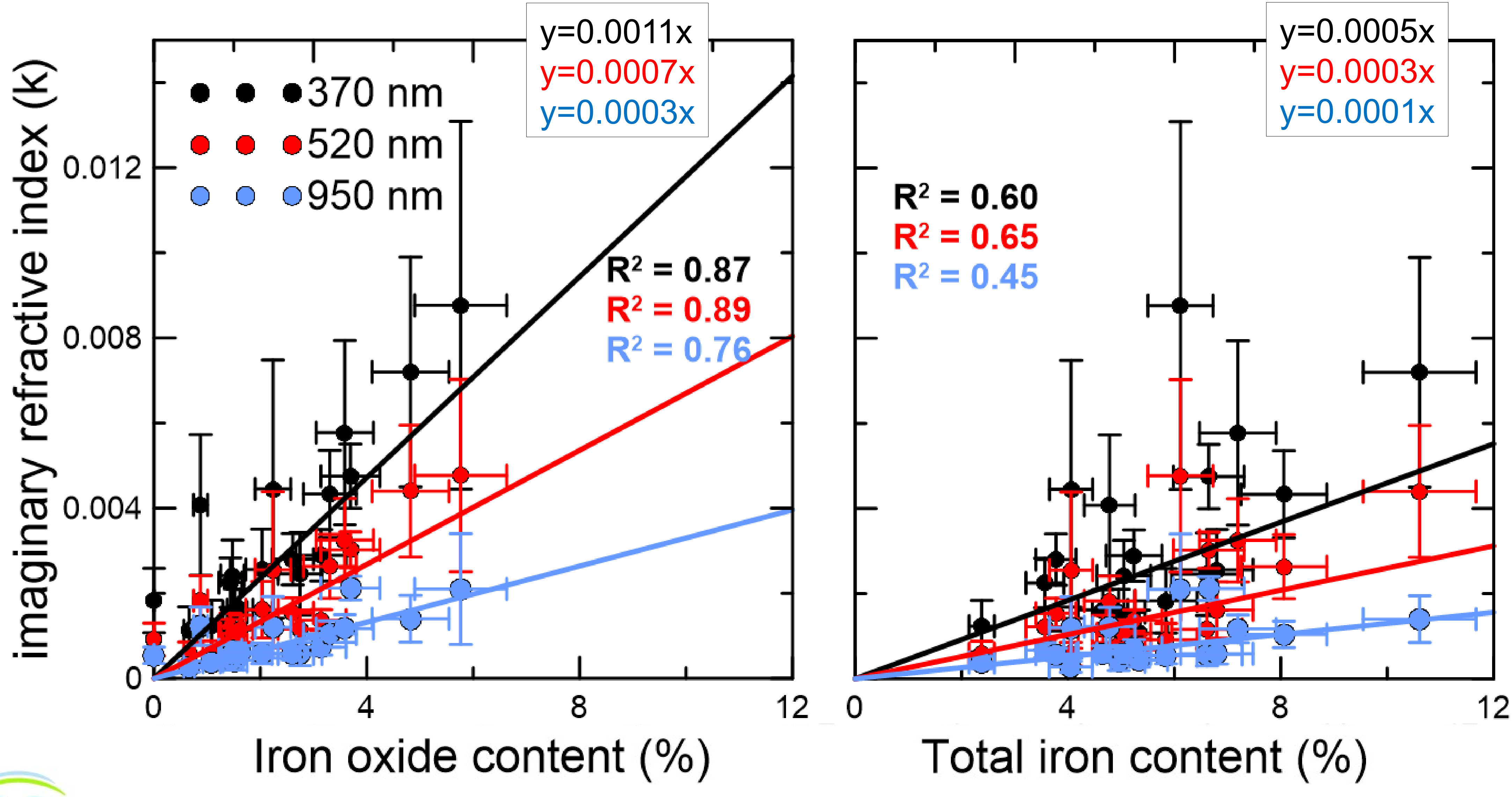

lisa cnrs

IR CRI vs mineralogy

CALCITE BANDS

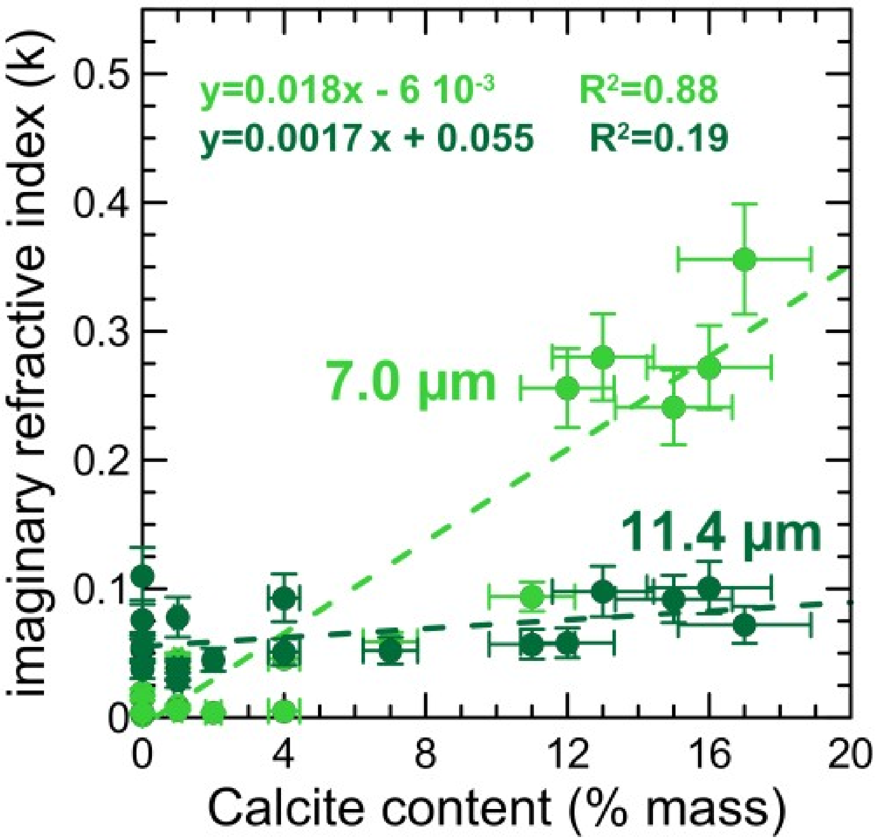

QUARTZ BAND

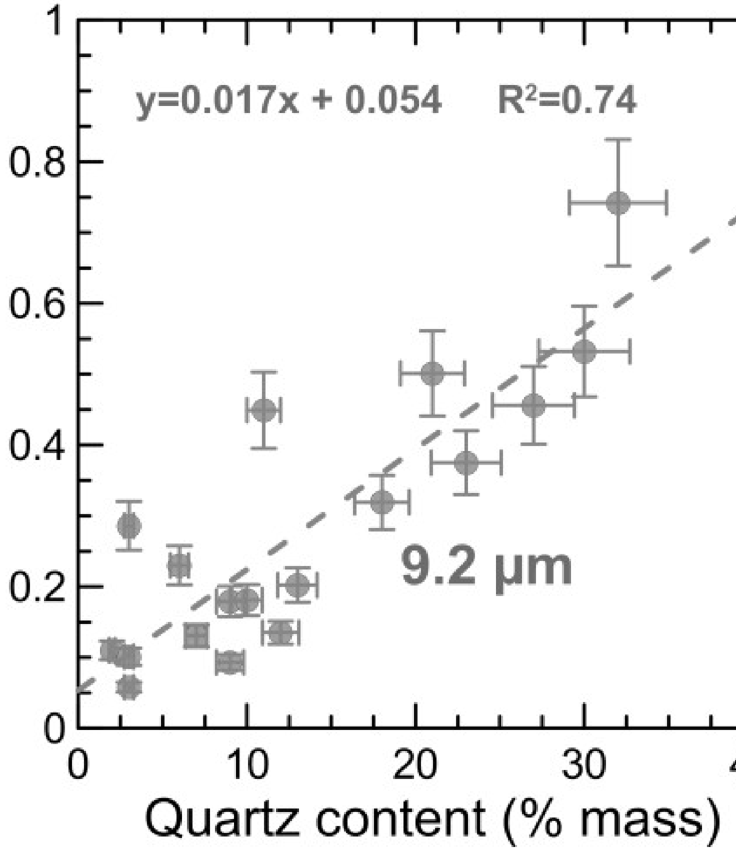

CLAY BAND

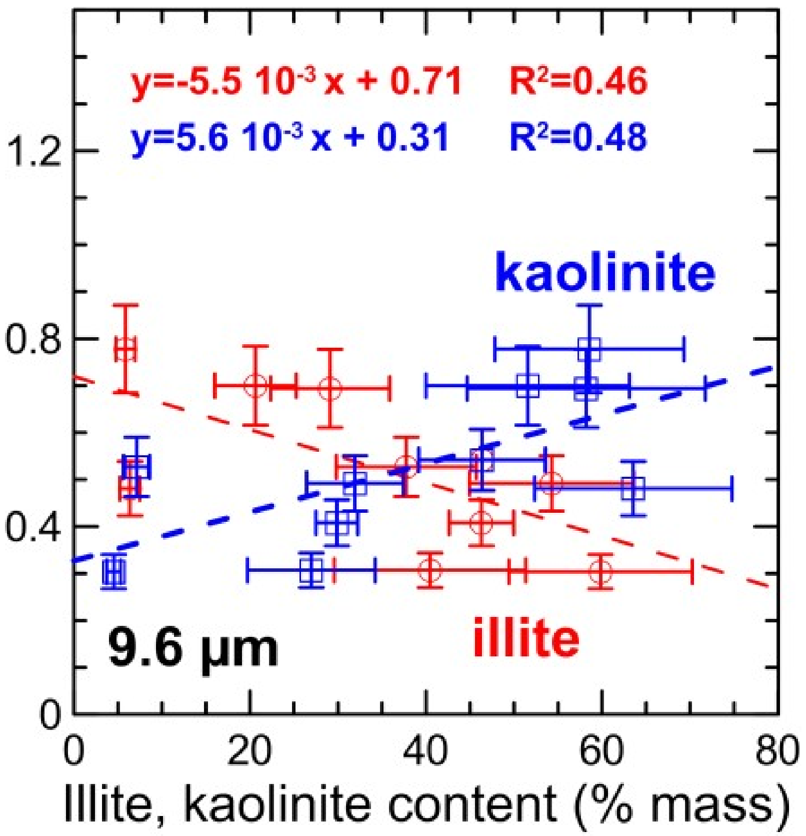

Ways forward

- Account the size-dependent mineralogy when calculating the optical properties – uses an aerodynamic aerosol classifier
- Account particle asphericity when measuring particle size (Huang et al., 2021; Formenti et al., ESSD, submitted)

CLImate relevant processing of Mineral Dust by volatile Organic compounds

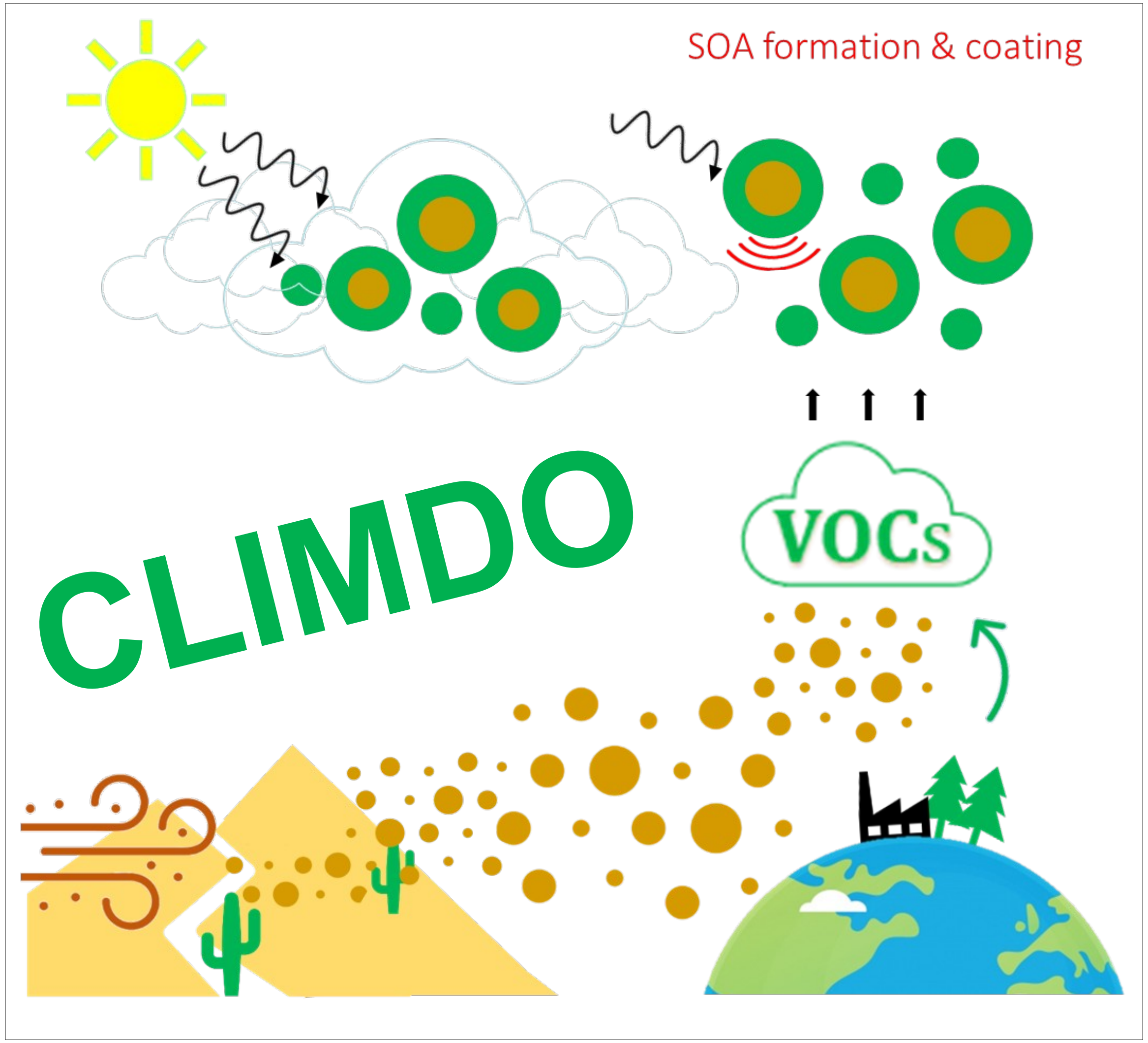

One limiting factor

Availability of soil samples for laboratory experiments

Thank you!

Relationship between SSA with iron and iron oxide content

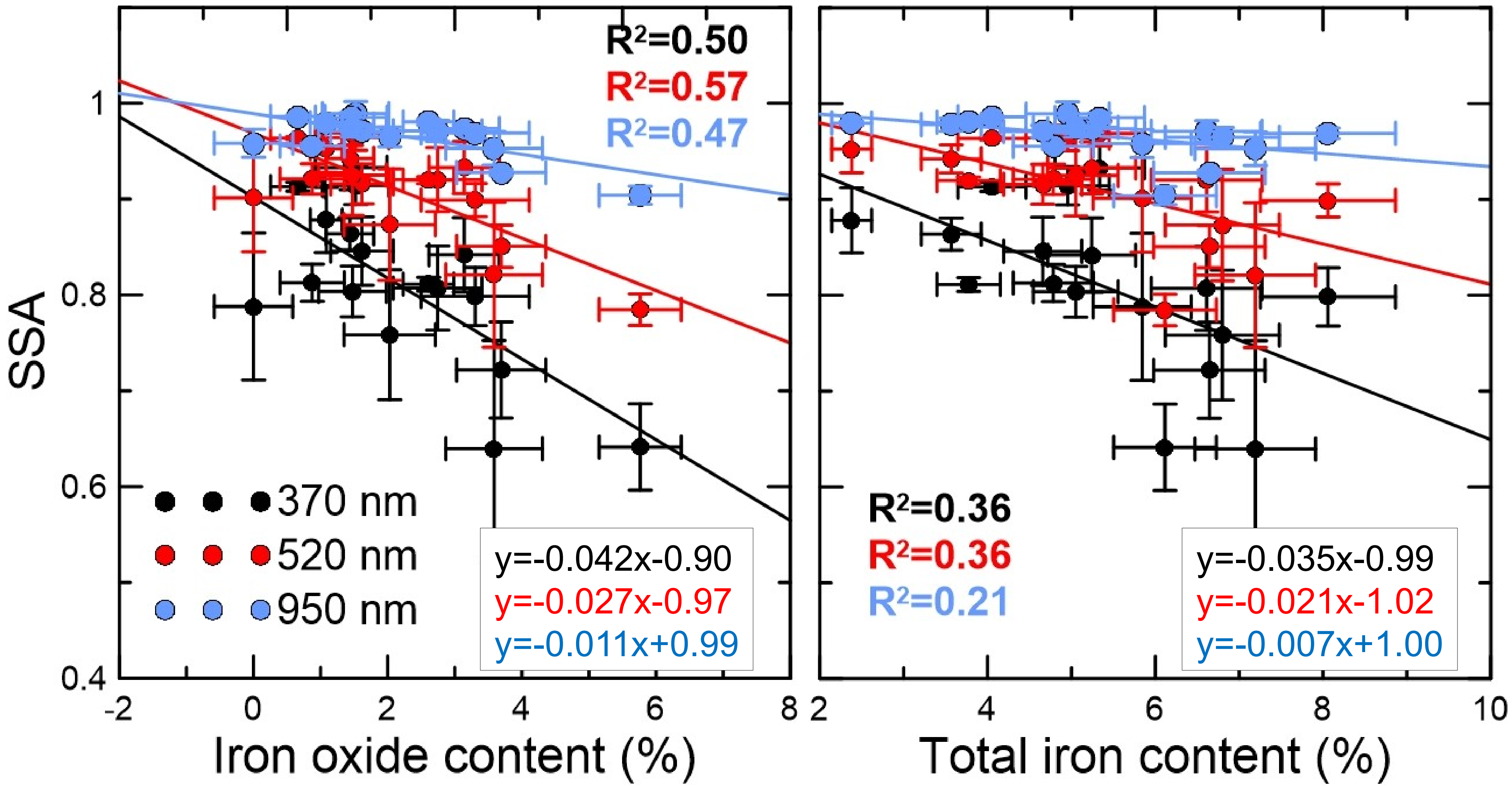

lisa

Dependence on the coarse size fraction

10-min (±1σ) values per experiment with $D_{eff,coarse}$ between 2 and 4 µm

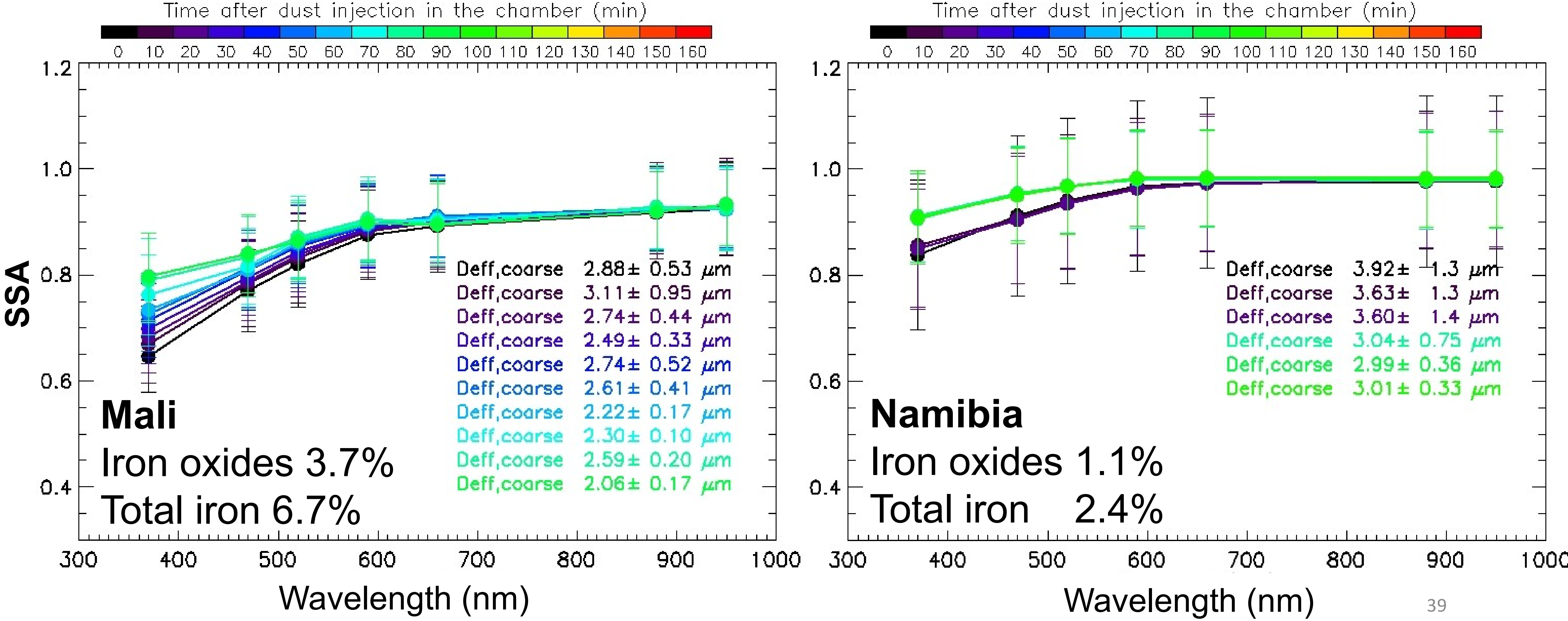

Experimental simulations

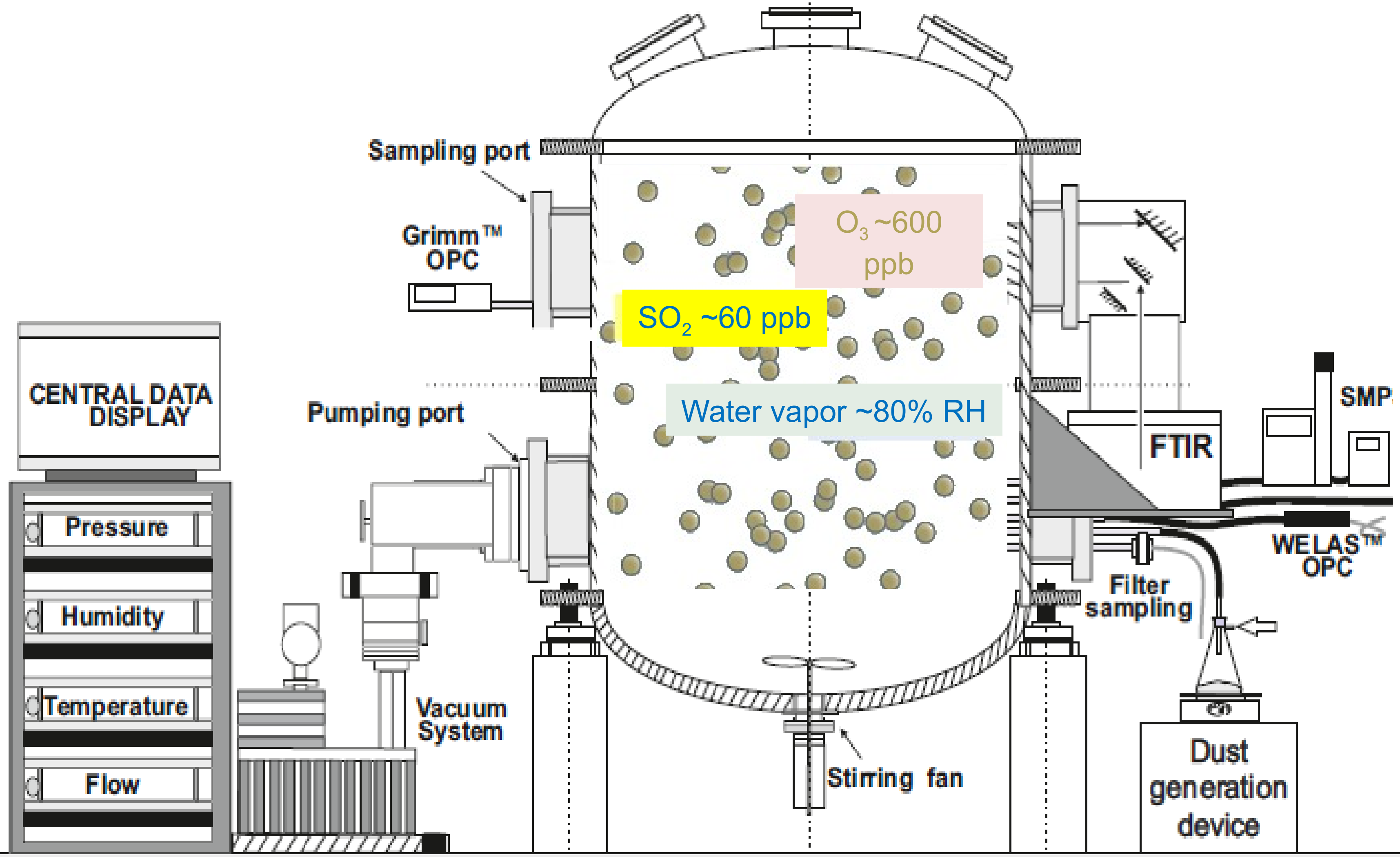

www.cesam.cnrs.fr

authentic mineral dust generated from natural soils

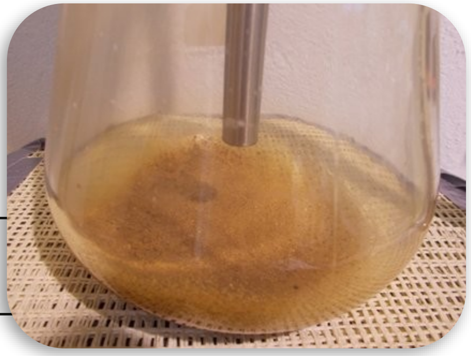

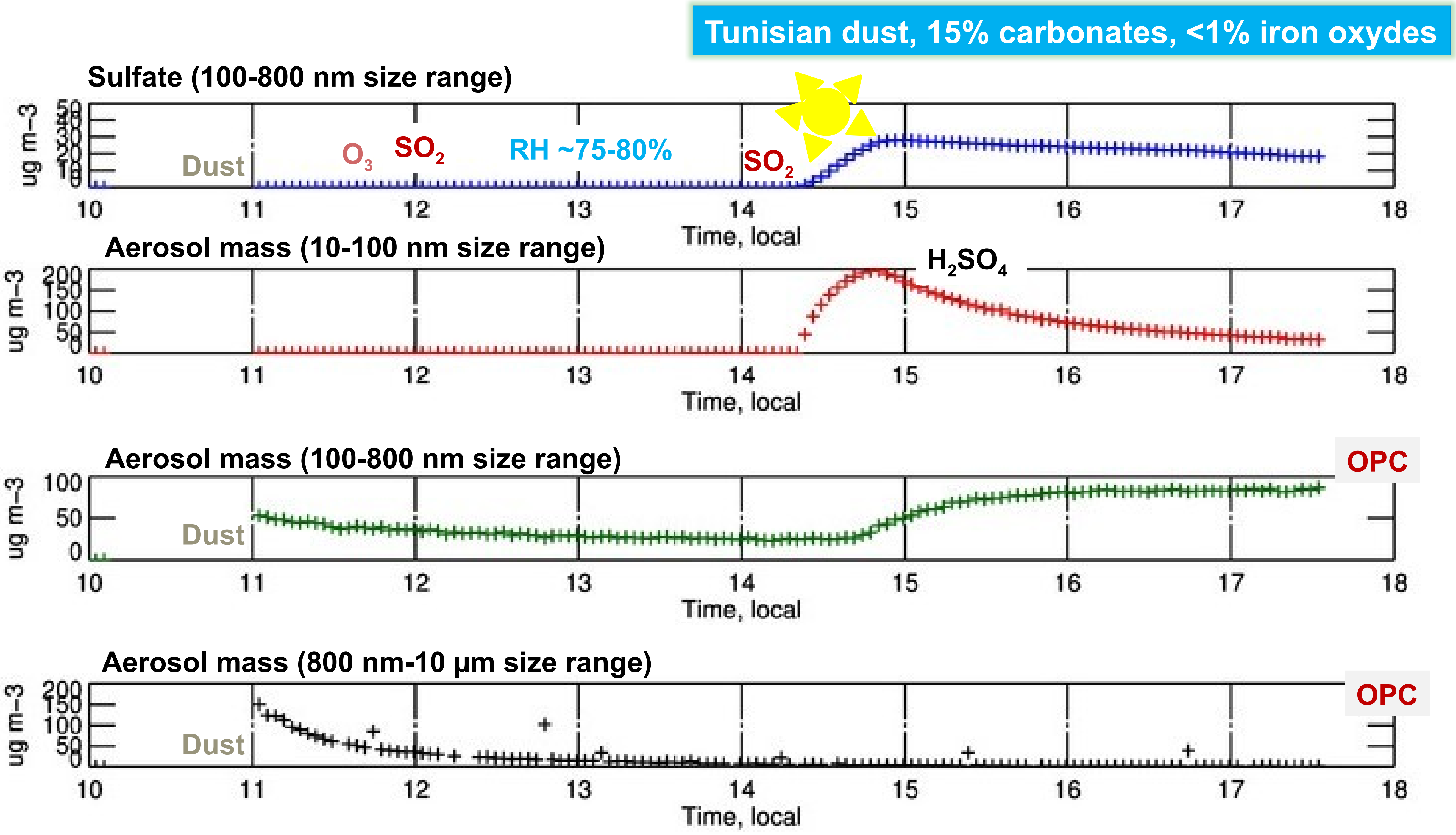

Tunisian dust, 15% carbonates, <1% iron oxydes
Sulfate (100-800 nm size range)
ug m−3
Dust
O_3
SO_2
RH ~75-80%
SO_2
Time, local
Aerosol mass (10-100 nm size range)
H_2SO_4
Time, local
Aerosol mass (100-800 nm size range)
OPC
Dust
Time, local
Aerosol mass (800 nm-10 µm size range)
OPC
Dust
Time, local

Representation of the size

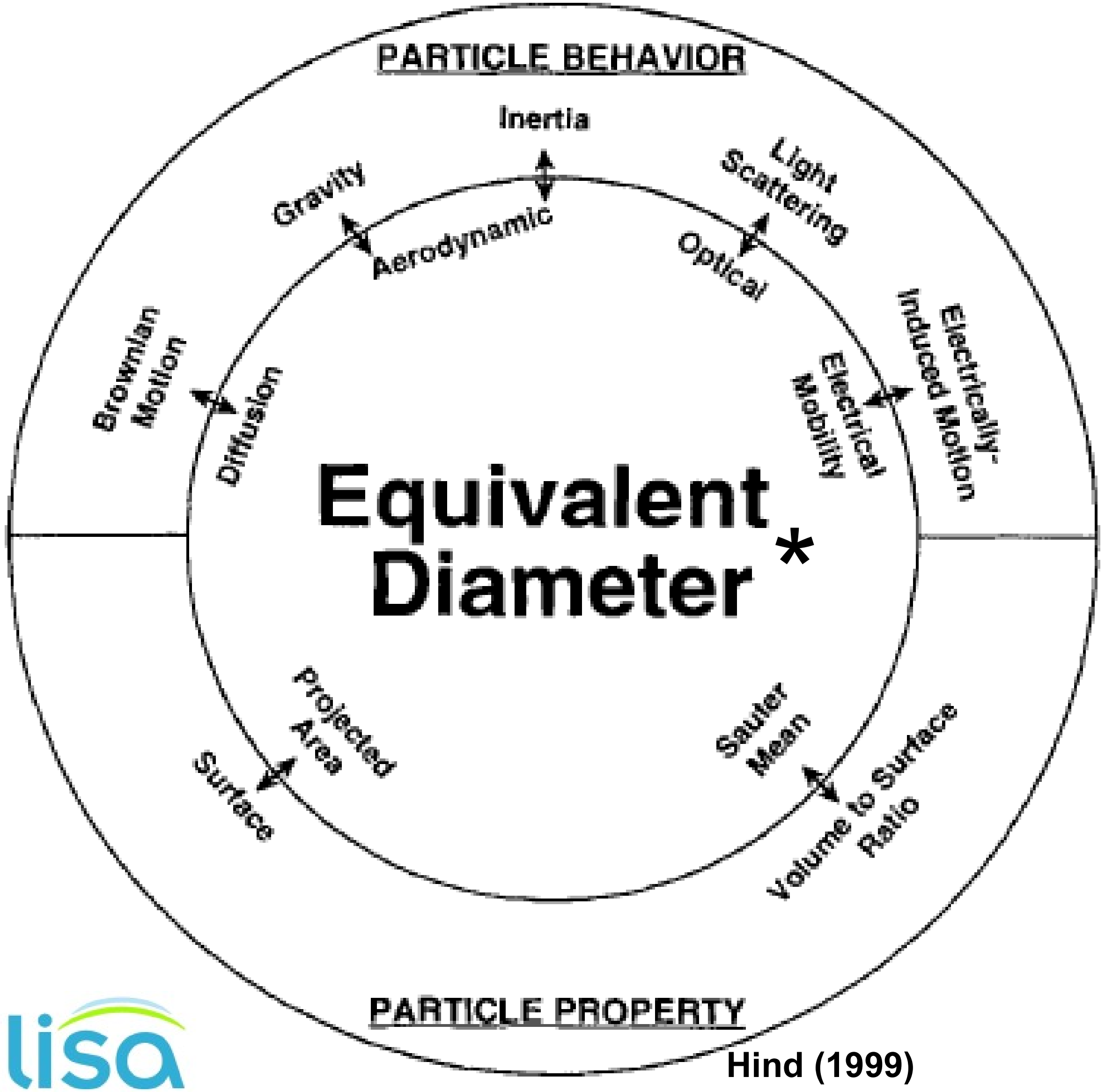

Hind (1999)

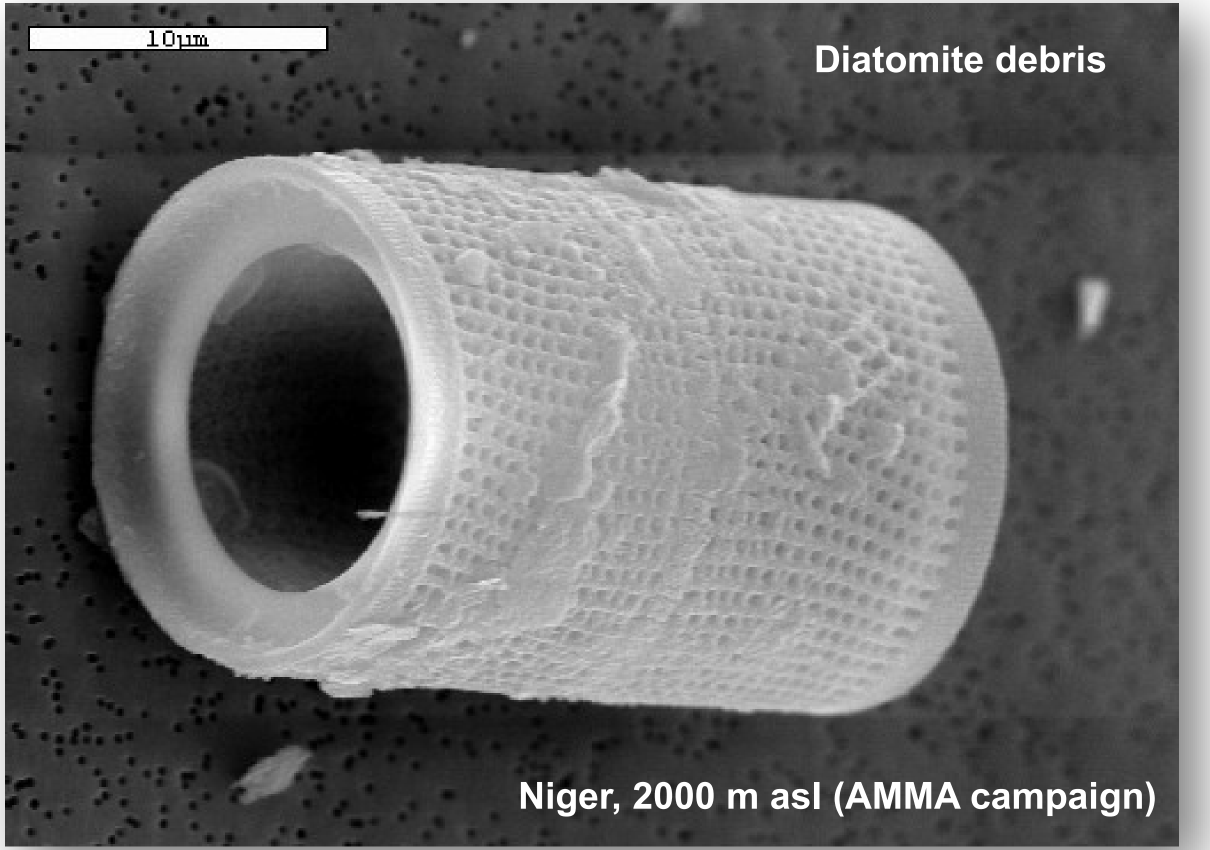

* depends on composition too

Geometric sizing - Morphology, Mineralogy

Off-line method; requires sampling of dust particles on appropriate substrates; samples are analysed by microscopy techniques.

Aerodynamic sizing - Mechanical behaviour

On-line methods; accelerates particles in an air stream and measures properties, which are proportional to the aerodynamic diameter.

Light Scattering - Optical / radiative properties

On-line method; measures the light scattered by particles at a given instrument geometry; scattered light is related to particle size for a calibration particle of spherical shape and known refractive index.

Optical Inversion Methods - Radiative properties

Off-line method; retrieves the effective diameter of an aerosol from remote sensing data on spectral extinction and angular scattering information, delivers column-integrated data.

adapted from Petzold (2008)

Long-range transported dust - PRIDE experiment

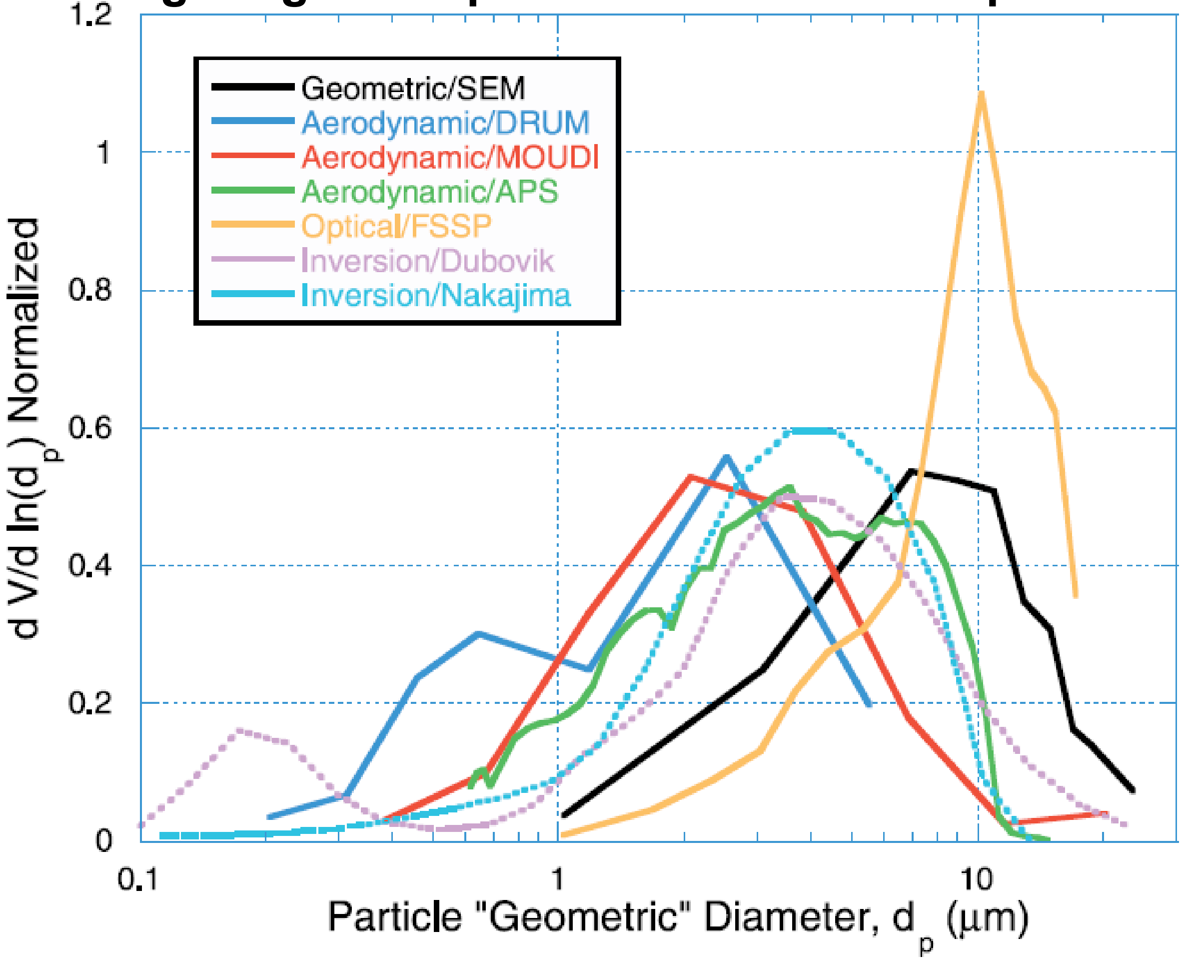

Reid et al. (2003)

Aerosol sizing

Geometric sizing - Morphology, Mineralogy

Off-line method; requires sampling of dust particles on appropriate substrates; samples are analysed by microscopy techniques.

Aerodynamic sizing - Mechanical behaviour

On-line methods; accelerates particles in an air stream and measures properties, which are proportional to the aerodynamic diameter.

Light Scattering - Optical / radiative properties

On-line method; measures the light scattered by particles at a given instrument geometry; scattered light is related to particle size for a calibration particle of spherical shape and known refractive index.

Optical Inversion Methods - Radiative properties

Off-line method; retrieves the effective diameter of an aerosol from remote sensing data on spectral extinction and angular scattering information, delivers column-integrated data.

adapted from Petzold (2008)

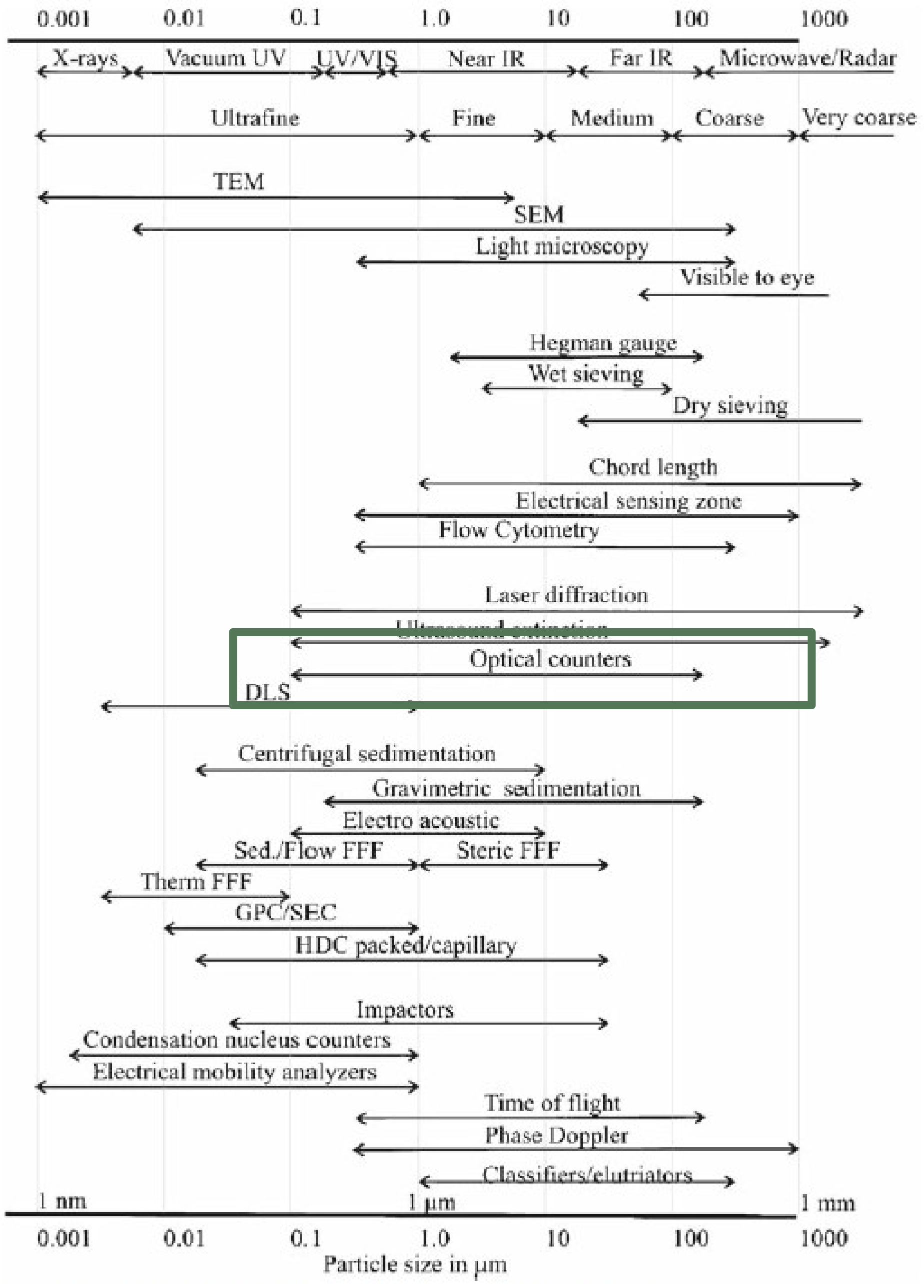

Fig. 3.1 Typical over-all measurement ranges of PSD techniques

Merkus, 2009

Huang, Y., Adebiyi, A. A., Formenti, P., & Kok, J. F. (2021). Linking the different diameter types of aspherical desert dust indicates that models underestimate coarse dust emission, Geophys. Res. Lett., 48, e2020GL092054, https://doi.org/10.1029/2020GL092054

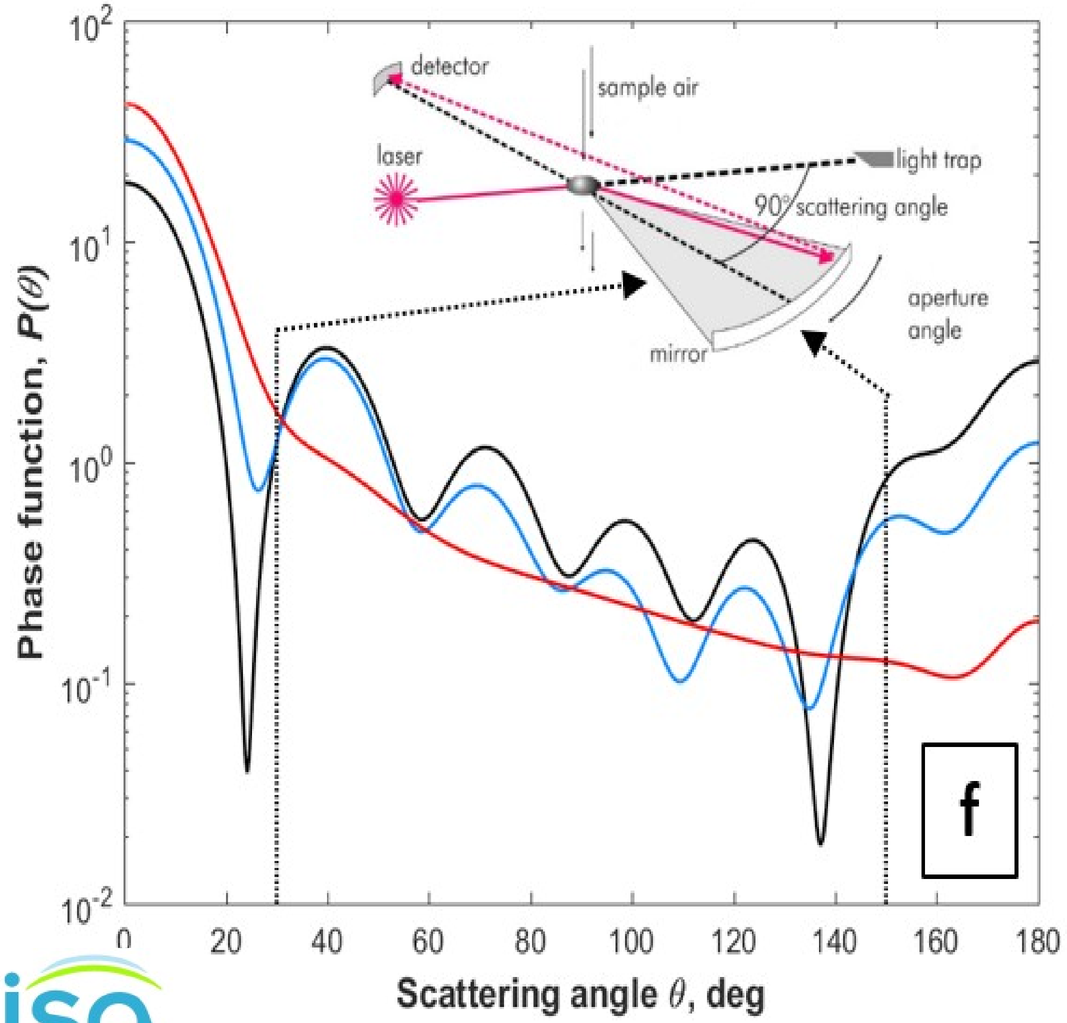

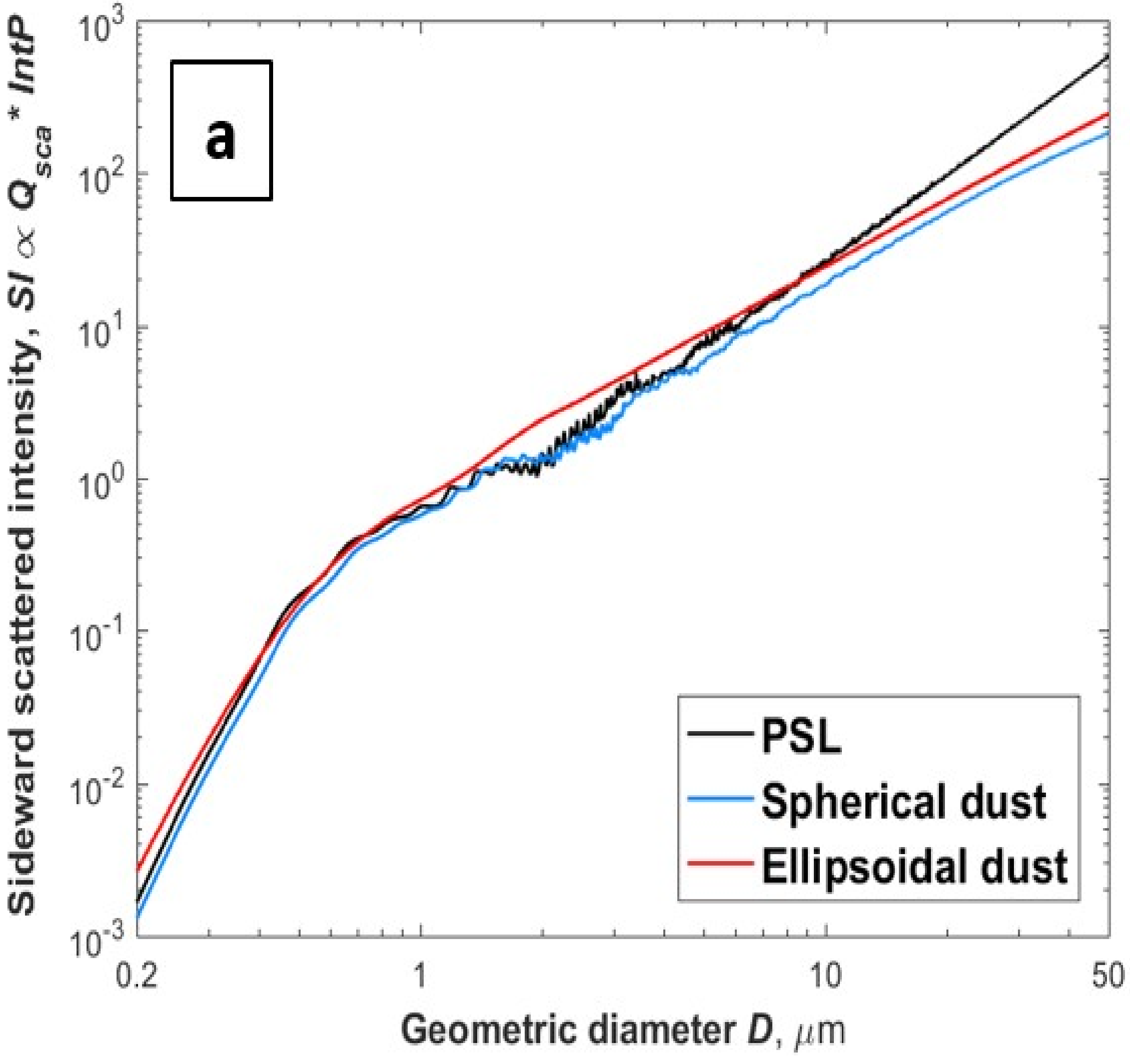

Huang, Y., Adebiyi, A. A., Formenti, P., & Kok, J. F. (2021). Linking the different diameter types of aspherical desert dust indicates that models underestimate coarse dust emission, Geophys. Res. Lett., 48, e2020GL092054, https://doi.org/10.1029/2020GL092054

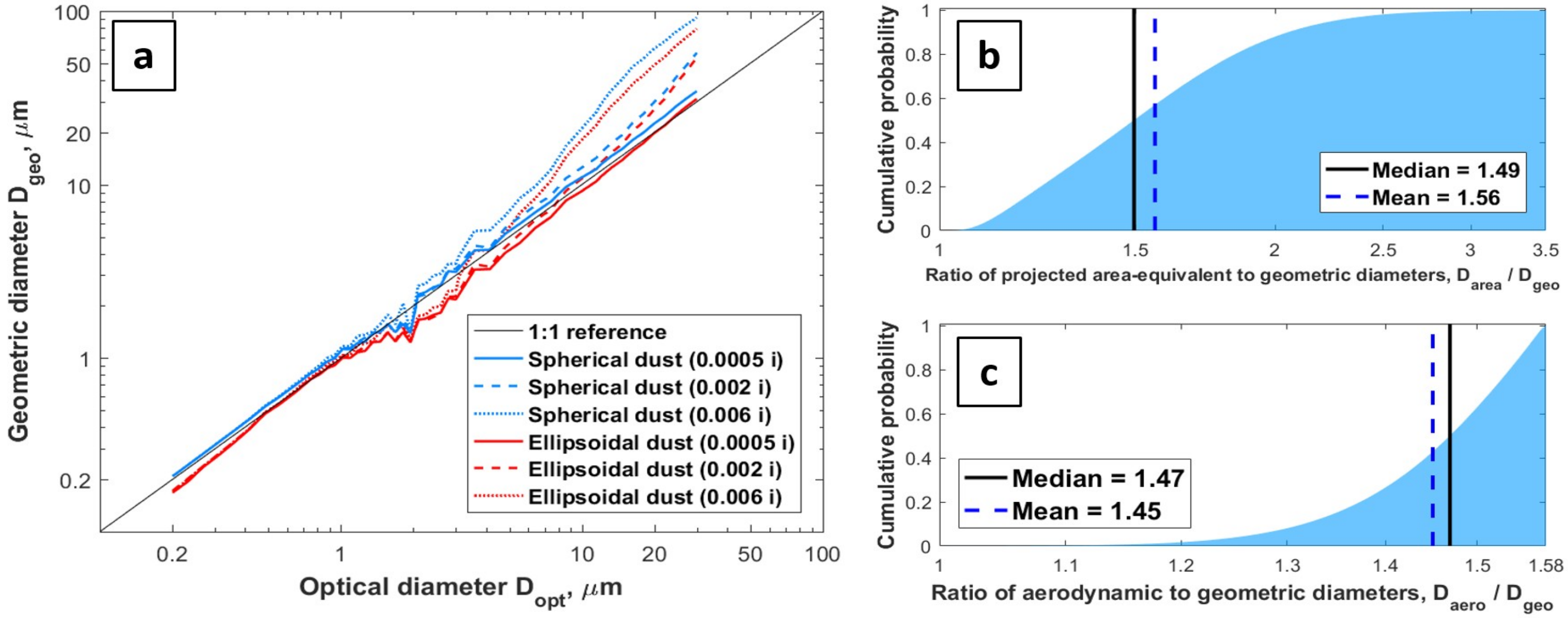

Figure 1. Conversion factors linking the four different diameter types of aspherical dust. Shown are (a) size-dependent conversions between the geometric and optical diameters, and size-invariant conversions between (b) the projected area-equivalent and geometric diameters, and between (c) the aerodynamic and geometric diameters. All three plots account for dust asphericity using the globally representative shape distributions detailed in Section 2.1. In panel (a), the OPC wavelength is taken as 780 nm, the scattering angle range is , and the real part of dust refractive index is 1.52. When the imaginary part increases from to and , the intersection optical diameters of red lines and the 1:1 reference line decrease from , to , and . Sensitivity tests of the conversions between the geometric and optical diameters to real and imaginary dust refractive indices, wavelength, and scattering angle range are shown in Supplementary Figures S1-S4, respectively.

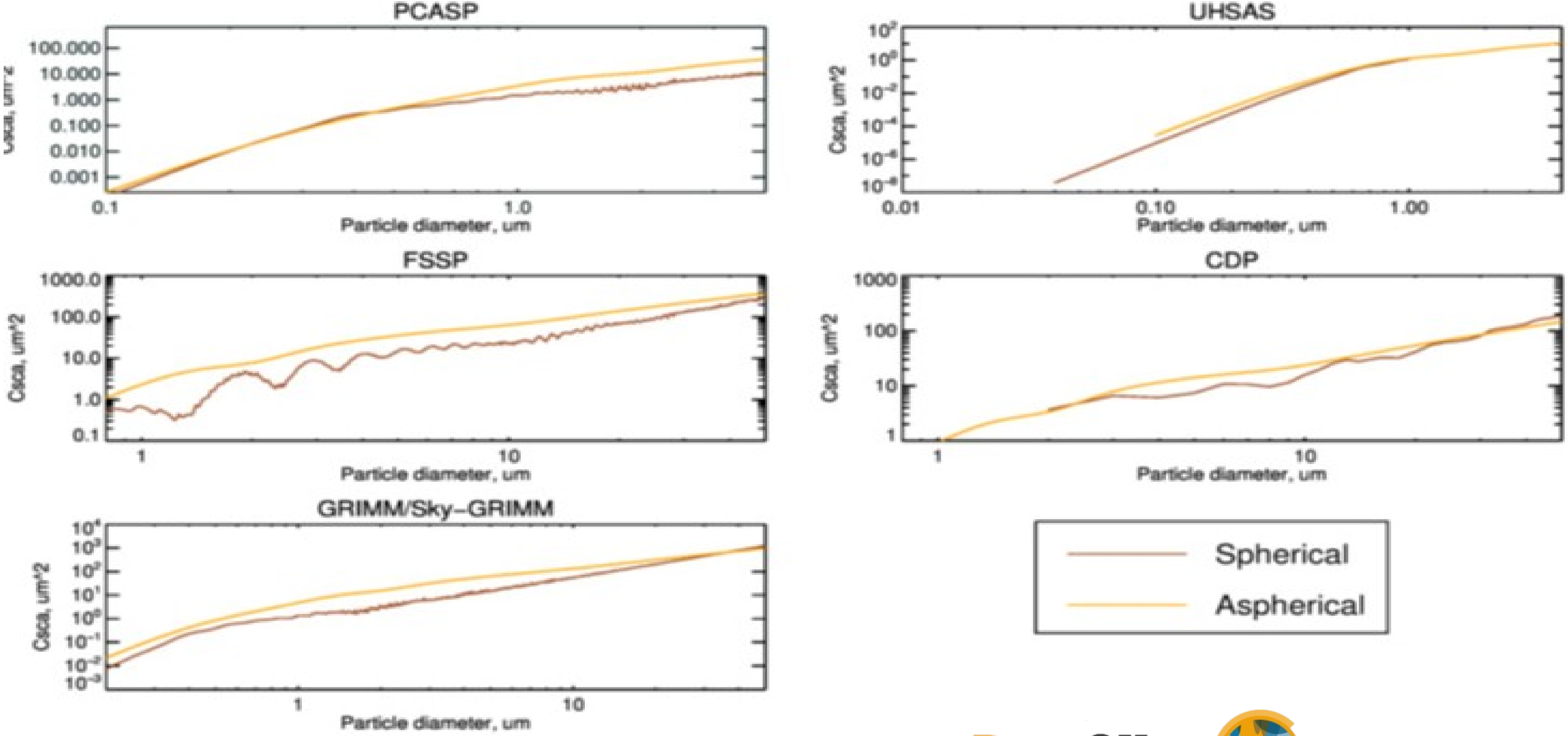

Figure 2. Scattering cross sections Csca as a function of particle diameter for the OPC considered in this paper moderately-absorbing mineral dust (CRI = 1.53 – 0.0032i). The brown line represents Csca calculated by Mie theory assuming homogeneous … l particles while the orange line represents Csca calculated … g to Huang et al. (2021) assuming homogeneous …al ellipsoid particles.

Formenti, et al, submitted to Earth System Science Data, essd-2021-292, 2021

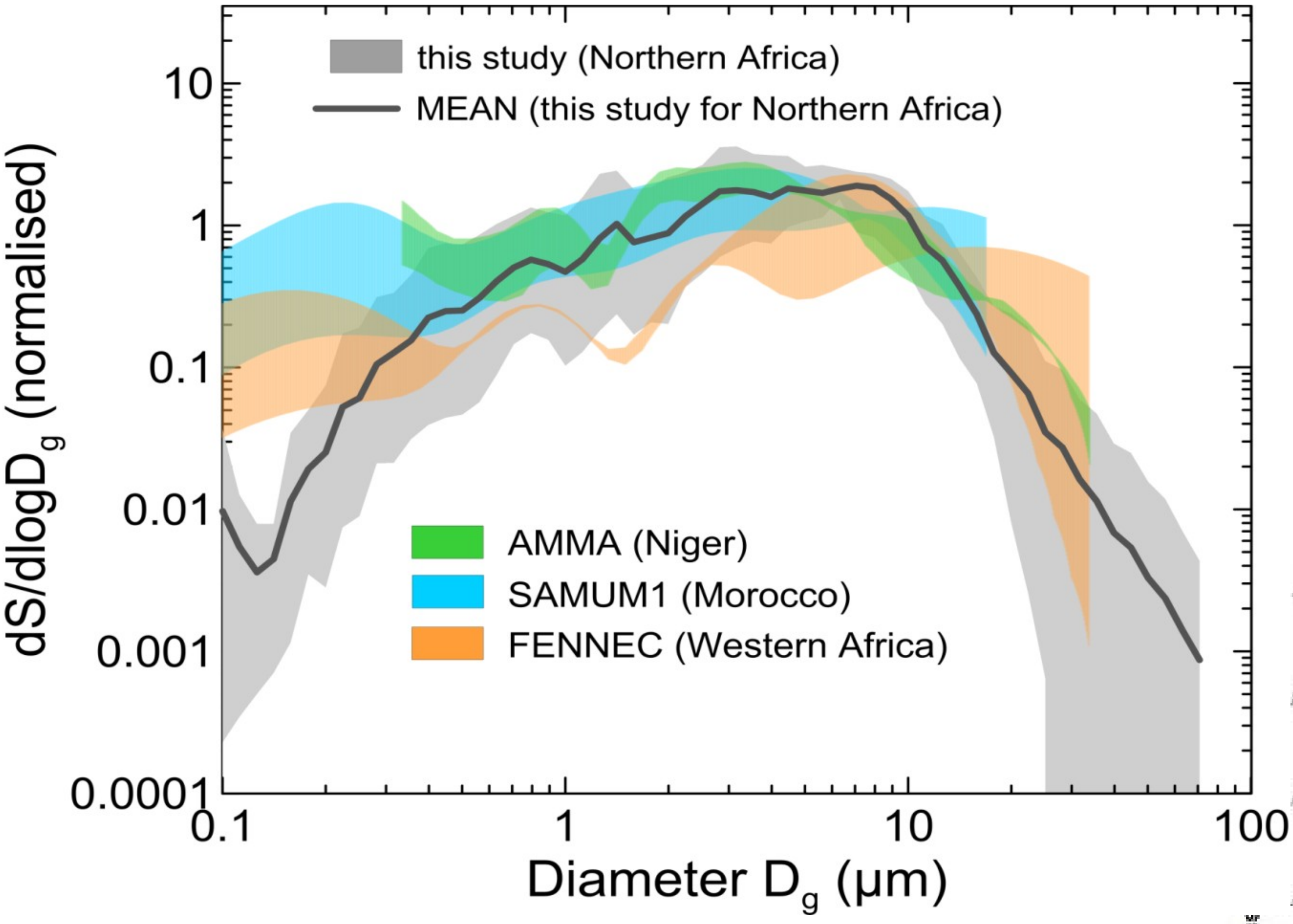
this study (Northern Africa)
MEAN (this study for Northern Africa)
AMMA (Niger)
SAMUM1 (Morocco)
FENNEC (Western Africa)
dS/dlogD$_g$ (normalised)
Diameter D$_g$ (μm)
10
1
0.1
0.01
0.001
0.0001
0.1
1
10
100

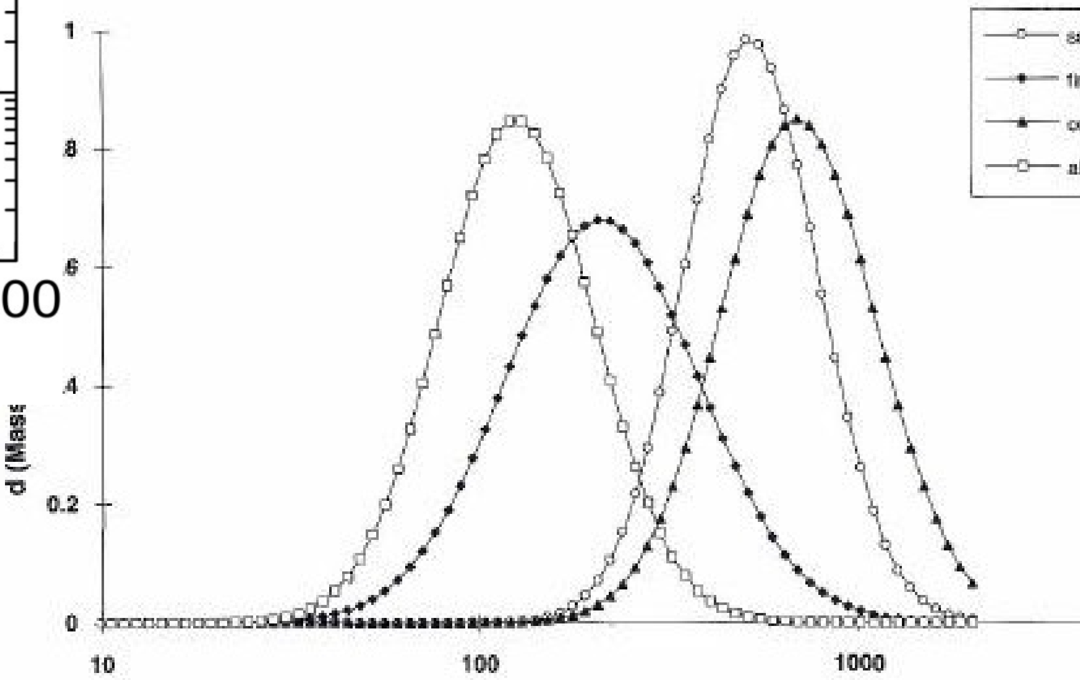
1
.8
.6
.4
0.2
0
10
100
1000

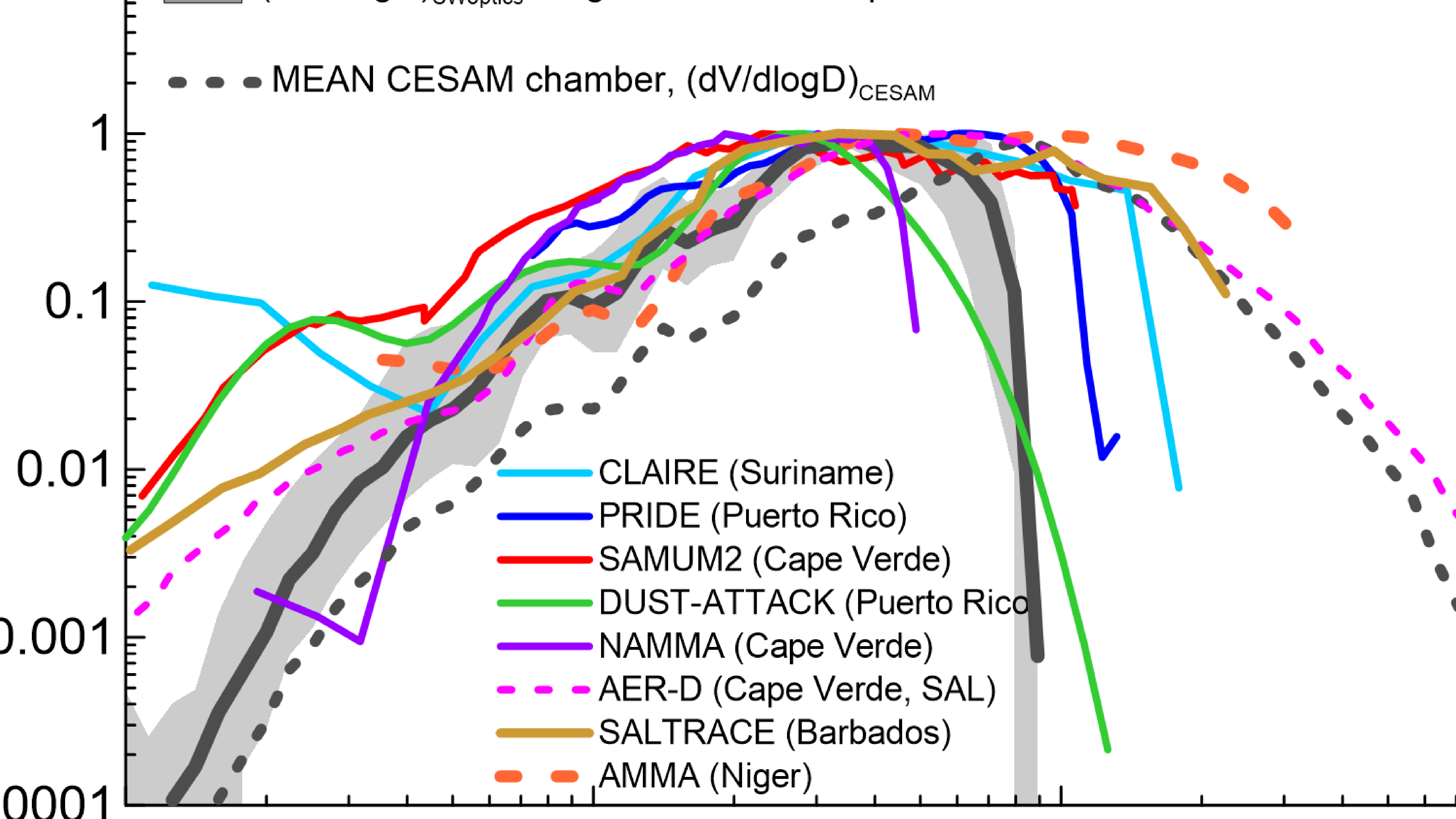

MEAN CESAM chamber, (dV/dlogD)$_{CESAM}$
1
0.1
0.01
0.001
CLAIRE (Suriname)
PRIDE (Puerto Rico)
SAMUM2 (Cape Verde)
DUST-ATTACK (Puerto Rico
NAMMA (Cape Verde)
AER-D (Cape Verde, SAL)
SALTRACE (Barbados)
AMMA (Niger)

A reference size distribution dataset

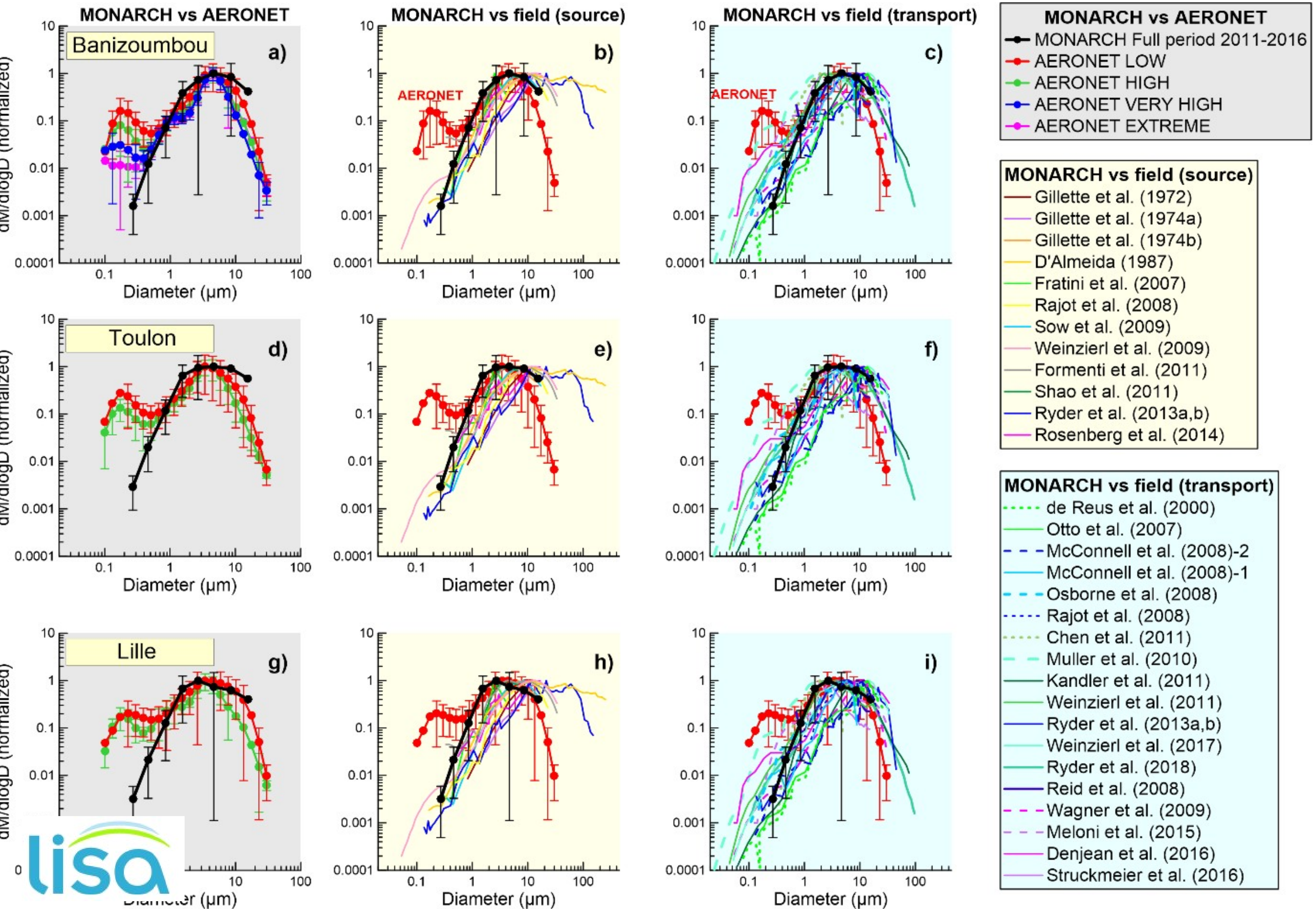

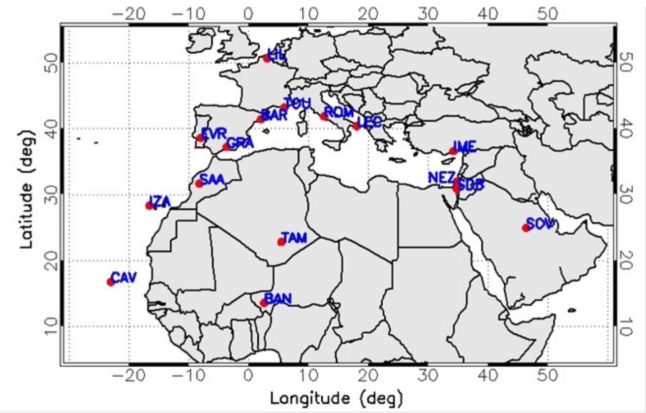

Formenti et al., in preparation for ESSD

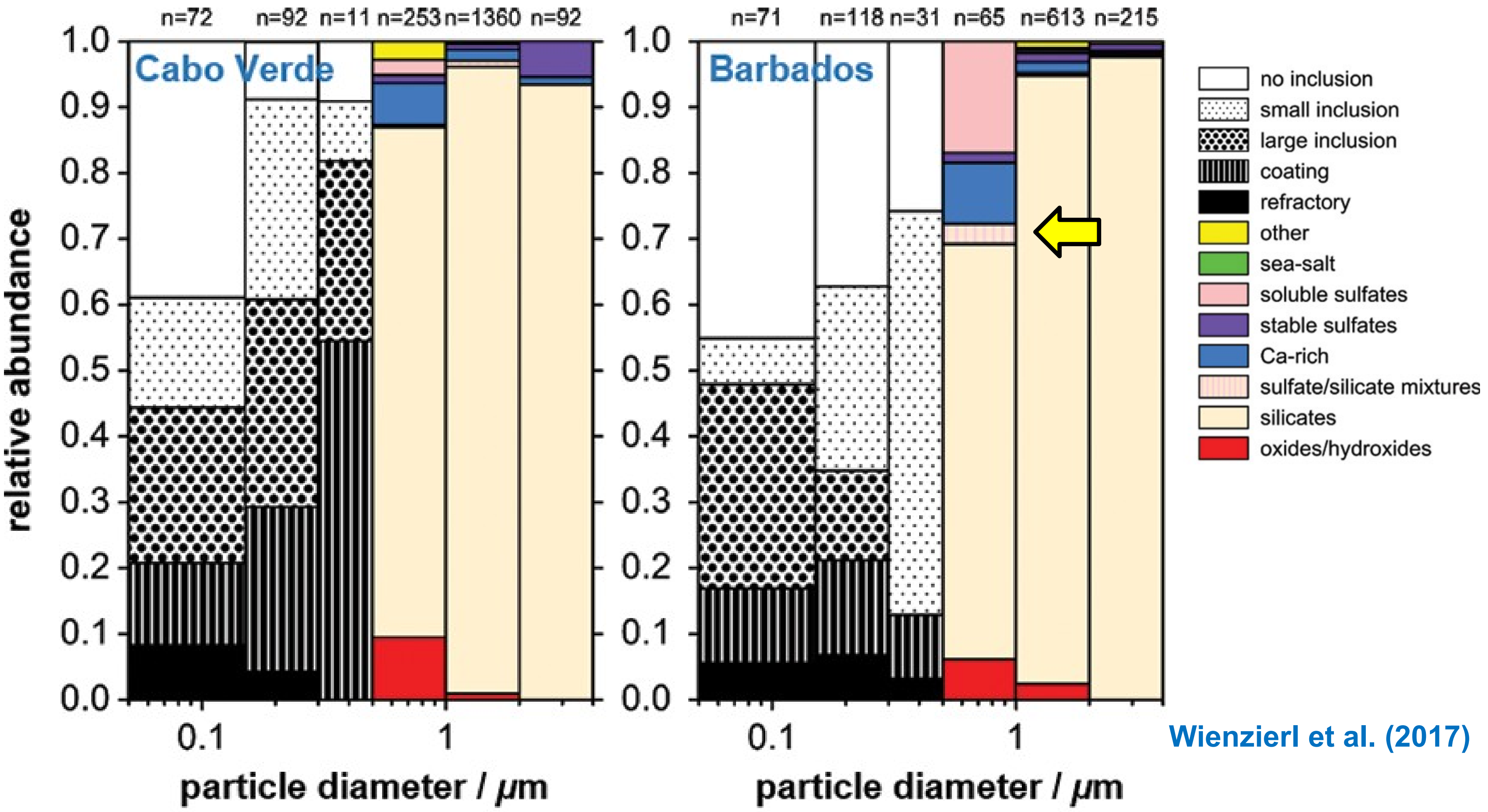

Wienzierl et al. (2017)

Also reported by Foner and Ganor, 1992; Ganor et al., 1998; Chabas and Lefevre, 2000; Formenti et al., 2001; Falkovich et al., 2001; Sobanska et al., 2003; Levin, 2005

Variabilité des propriétés optiques confirmé par les observations de terrain

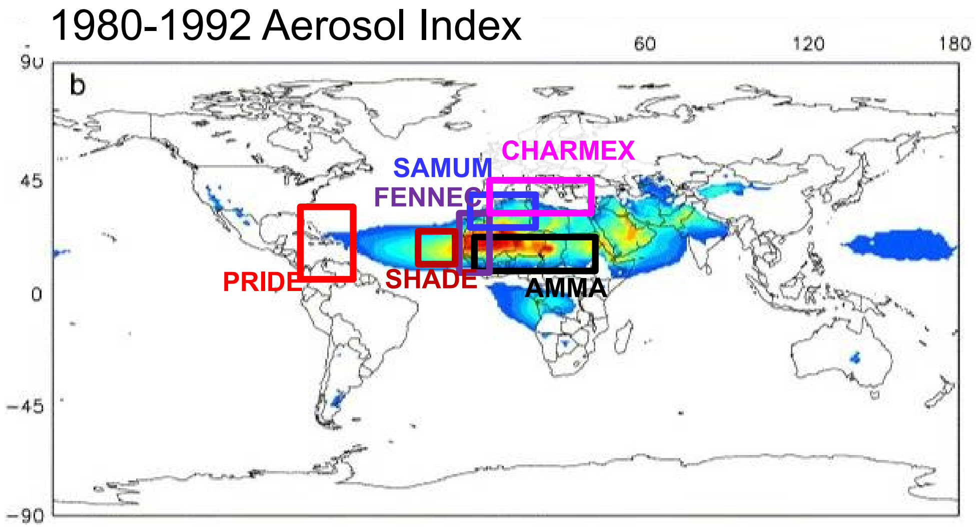

Domaine spectrale SW

SSA (500 nm) ~ 0.75-1.0

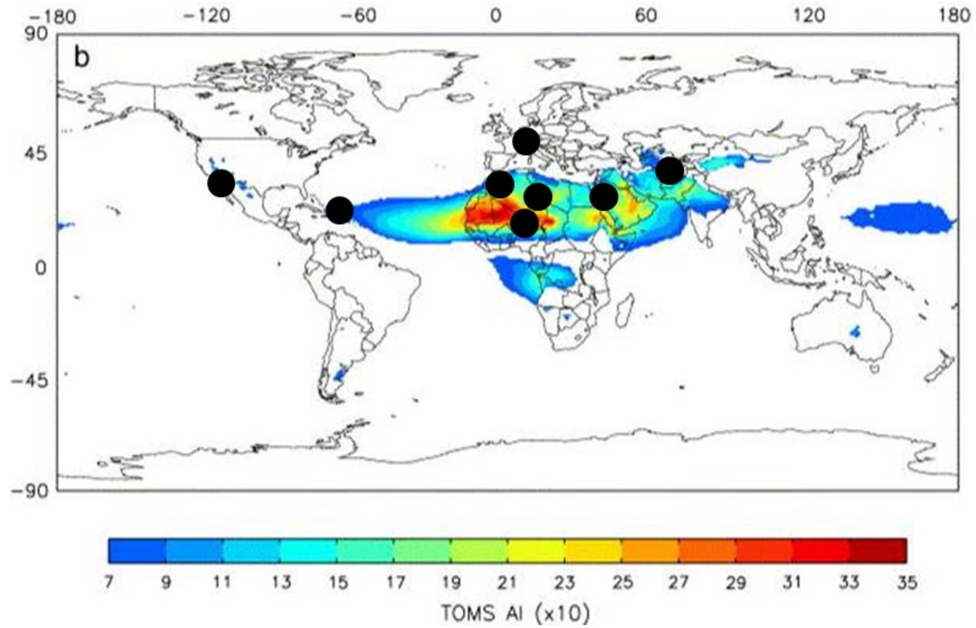

Domaine spectrale LW

SSA (10 µm) ~ 0.2-0.6

SSA= single scattering albedo

Dust extinction spectra

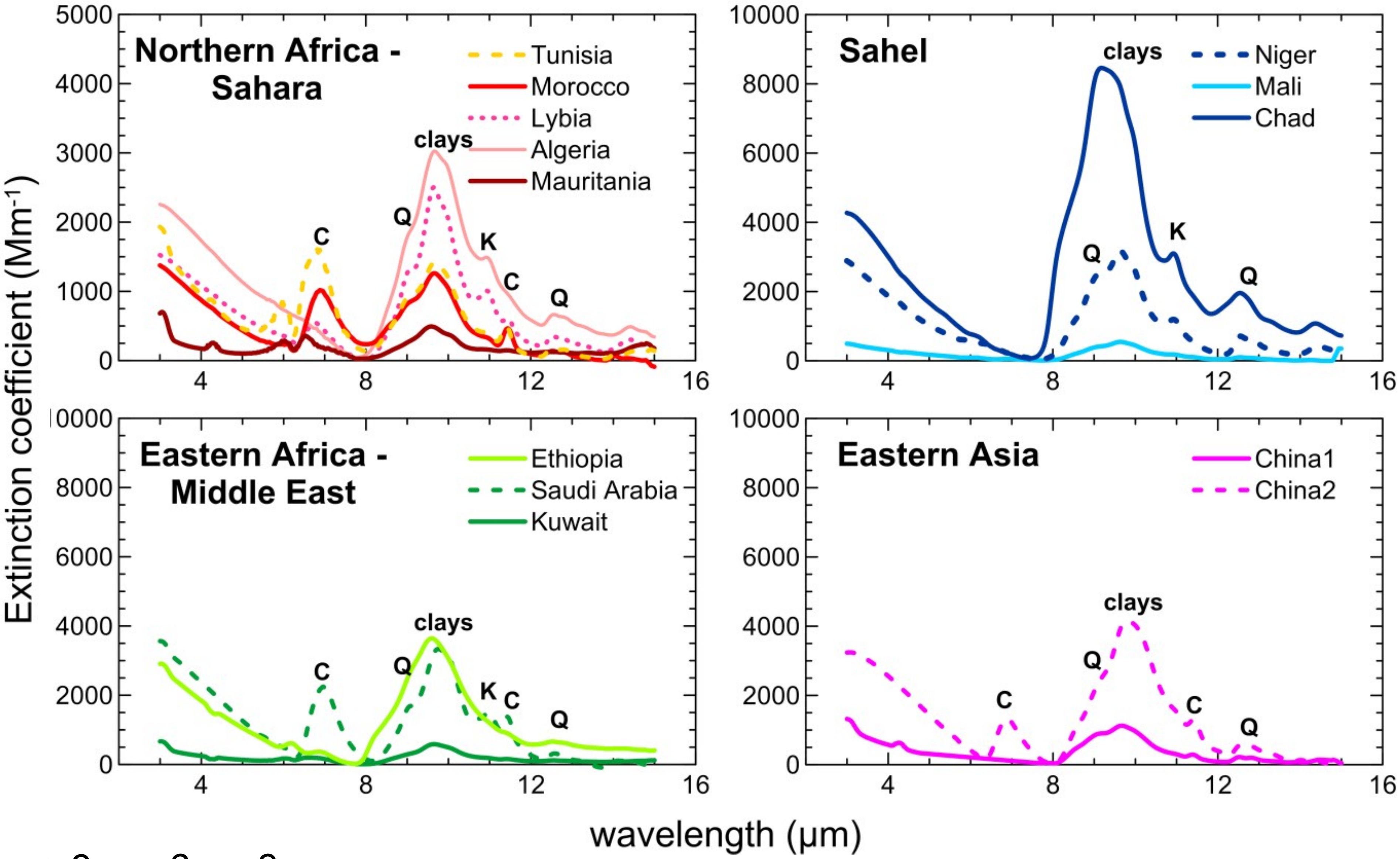

>6 µm $\beta_{ext} \sim \beta_{abs}$

Synthesis and comparison

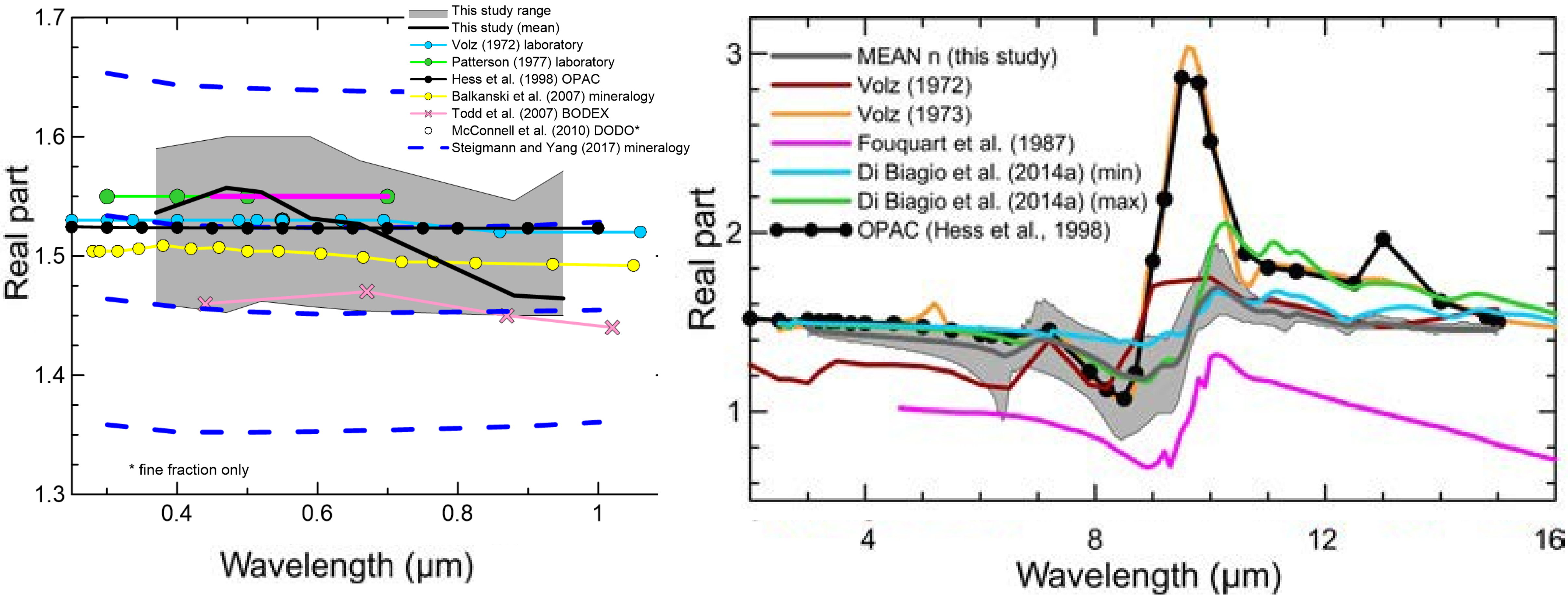

A relatively narrow range of values, little if no spectral dependence